Part II.

Modeling Hurricane Surge Physics

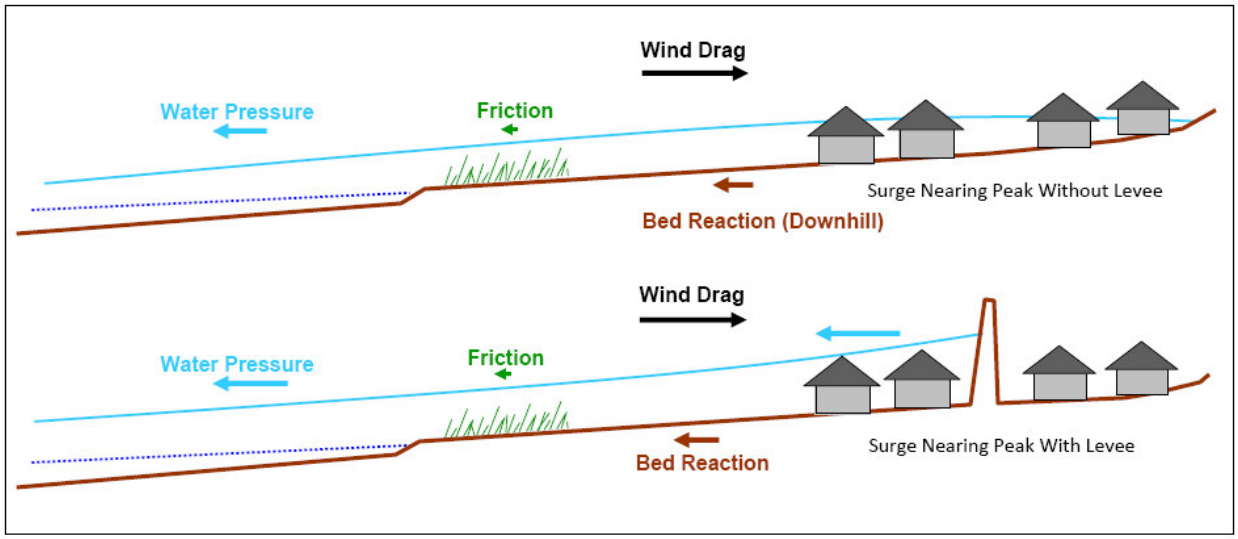

Subpart A. Hurricane Surge Physics

A hurricane reaches Category 3 or higher in the Gulf of Mexico, on average, every other year, with over 40 percent making landfall along a 500-mile stretch of the central-northern coast. These hurricanes possess a range of core intensities (indicated by the central pressure deficit and maximum eyewall winds), core sizes, wind field distributions, forward speeds, and tracks. Part I of this Report reviewed the current science on hurricane climatology of the CN-GoM. This information provides the basis for present return frequency estimates for hurricanes exhibiting various joint characteristics. For example, the landfall of storms with intensities at strong Category 3 and borderline Category 4-5 are estimated to have a return periods on the order of 40 and 212 years for a 1° latitude segment south of New Orleans LA (see Section 4).

The landfall of major hurricanes near the middle of this region—along the unique coastal conditions of southeast Louisiana—creates the most extreme surge inundation hazards in the United States, as typified by Hurricanes Betsy in 1965, Camille in 1969, and Katrina in 2005. This Part II, Subpart A reviews the scientific basis for these hazards by examining the three following subjects:

Section 5., the components of hurricane surge and the surge dynamics[1];

Section 6., the physics of hurricane surge;

Section 7., the interaction of hurricane surge with regional coastal landscape features; and

This subpart primarily provides a qualitative discussion of these concepts. Part II, Subpart B addresses surge hydrodynamic modeling—state-of-the-practice methods which can be used by risk managers to estimate surge dynamics for any specific hurricane. Part III then summarizes the approach to combining hurricane joint probabilities and surge modeling in analyzing hurricane surge hazards.

[1] *Surge dynamics* refers to the changing shape of the SWL surface during the course of hurricane landfall. This is distinguished from *coastal or landscape morphodynamics* which refers to changes in terrain and bathymetric features associated with the surge. Examples of landscape morphodynamics include barrier island and headland dune erosion, shoreline erosion, widening and deepening of coastal passes, expansion of shoals adjacent to passes, and loss of vegetation.

Section 5. Surge Components and Dynamics

5.1. Surge Components

As illustrated in Figure 5.1, surge is basically an extensive dome of water with surface waves. The dome is created primarily by the hurricane wind field acting on the water and secondarily by the storm's CPD (see Section 6). The surge dome typically extends many tens of miles—occasionally exceeding 100 miles—and its passage can take over a day along the open coast and longer for inundated areas and shelter water bodies. Figure 5.1 shows that as the storm approaches the coast and depths decline, the hurricane wind action produces a taller dome.

The elevation of the surge dome is compared to *Local Mean Sea Level (LMSL)* and *Local Monthly Mean Sea Level (LMMSL)*. LMSL is a very long-term (on the order of 19 year) average coastal sea surface elevation which factors out the effect of astronomical tide cycles, as well as short-term and seasonal meteorolological and hydrodynamic events. Gradual changes in the LMSL based on multi-decade gauge data can be used to estimate sea level rise. NOAA computes LMSL at coastal locations throughout the United States, including the CN-GoM. LMSL can also be estimated for inshore locations—such as coastal passes (e.g., Rigolets), lakes (e.g., Borgne and Pontchartrain.), bays (e.g., Barataria, Eloi), and sounds (e.g., Chandeleur, Breton, and Mississippi)—using long-term data from other (e.g., USGS, USACE) gauges. Using high quality local control information tide gauge data is converted to the North American Vertical Datum of 1988, in the appropriate epoch (see GTN-2 for a discussion of geoid vertical referencing). Stable regional coastal hydrodynamic factors—such as slight differences in gravity, river base inflow, and ocean currents create variations in LMSL referenced in NAVD88. LMSLs at Grand Isle LA and near West End in Lake Pontchartrain are 0.2 and 0.5 feet NAVD88-2006.81, respectively (NOAA 2011).

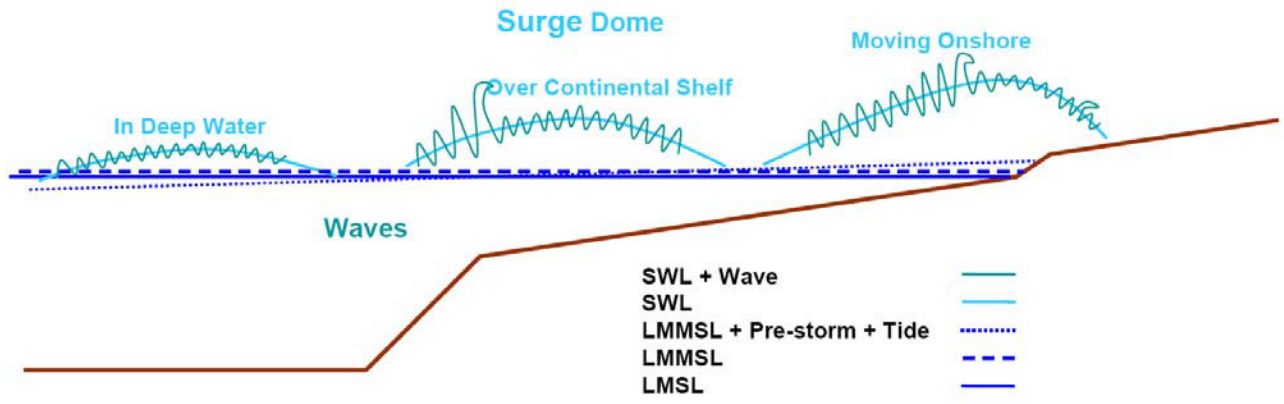

Figure 5.1. Typical Surge Components Moving From Deep Water to Onshore
(not to scale)

LMMSL is the average montly water surface elevation that would be present without the astronomical tides and individual short-term meteorological events. LMMSL reflects seasonal meteorological trends—e.g., regional runoff and persistent wind setup associated with frontal passages or centers of low/high barometric pressure—and steric effects (thermal expansion/contraction of Gulf of Mexico sea water). During late summer/early fall the LMMSL along the southeast Louisiana coast is about six inches above the LMSL. (USACE 2008). Computation of a LMMSL also requires gauge data for many years.

Along coastal southeast Louisiana astronomical tides are dominated by the diurnal (daily) as opposed to semi-diurnal (twice daily) gravitational affects of the sun and moon acting on the ocean waters, and highly dampened compared to the Atlantic coast. Six major constituents include the K_1, O_1, Q_1, and P_1 diurnal and the M_2 and S_2 semi-diurnal constituents. Amplitudes (and phases) have been established by NOAA from long-term tide station data. For example at a Shell Beach LA in Lake Borgne 0.453, 0.42, 0.085, 0.138, 0.079, 0.062, or a total of just over 1.2 ft (NOAA Tides and Currents). The southeast Louisiana tide range can exceed 2.5 ft along the open coast and up to 6 inches in Lake Pontchartrain.

Figure 5.2 illustrates gauge data for one month at Grand Isle LA. The figure shows the predicted astronomical tide (blue), observed gauge data with tides (red), and the data with tides filtered out (green). The tide-filtered stage shows the influence of non-tropical weather events. Factoring in tides, seasonal effects, and the occasional non-tropical weather event generating strong coastal winds, the local sea level along coastal southeast Louisiana at any time typically ranges within ±3 ft of LMSL.

Together, the LMMSL, astronomical tide, pre-storm influence, and the surge dome, are called the *storm tide*. The measured elevation of the storm tide or *total surge* (referred to henceforth as simply surge) is termed the *still water level* (SWL) because it removes the influence of high frequency waves. [Wave scientists often use SWL to refer to a totally undisturbed water surface—e.g., in an experimental flume prior to creation of waves—and mean water level (MWL) to refer to the wave-filtered elevation at any point. However, hydrologists use the term "still," as in SWL, to simply refer to the wave-filtered level.]

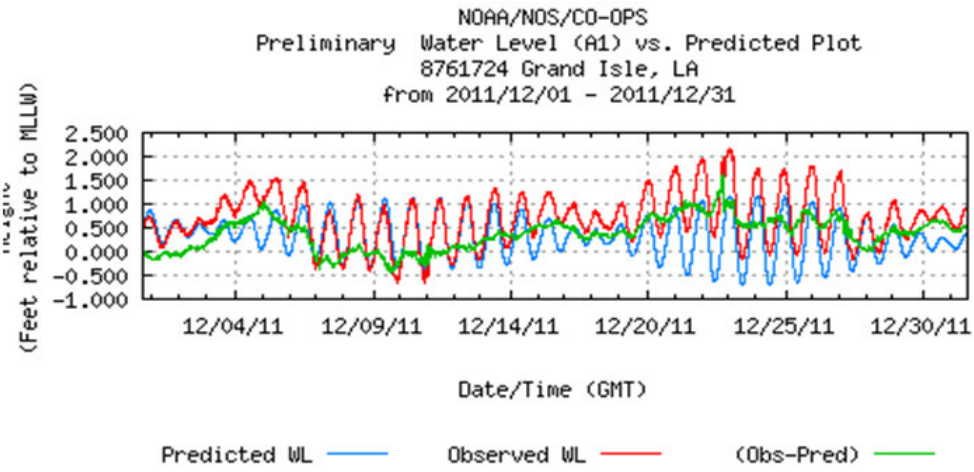

Figure 5.2. Example of Tides Filtered Out from Daily Tide Gauge Data
NOAA 2011

SWL data can be obtained from stage data recorded with the use of stilling basin or from data that is smoothed (i.e., with high-frequency waves filtered out). The red lines on the two NOAA graphs in Figure 5.3 illustrate surge SWL data (the green line is the astronomical tide component). Overland SWL measurements can be derived from post-storm high water marks (HWMs) within building interiors. As illustrated in Figure 5.3, for an extreme hurricane such as Katrina, the peak two feet of surge lasts for many hours on the open coast and for a few hours along interior lakes and bays, (but longer in confined areas where receding is delayed).

The high-frequency waves have periods measured in seconds and oscillate about the SWL as shown in Figure 5.1. The wavelengths are measured from peak to peak (the period is the time required for passage of one wave, peak to peak) and heights are measured from trough to peak. Offshore wave lengths are much greater than heights and waves are nearly symmetric about the SWL (approximating a sine function). With shoaling wave heights increase and lengths decrease. With the approaching shoreline, as depth (SWL minus the bathymetric elevation) continues to decline below increasing wave height, waves become increasingly steep and asymmetric until they break. Thus, in the nearshore and over inundated areas the surge depth controls the maximum height of waves, and the greatest wave heights generally, but not always, occur with maximum SWL.

Different wave conditions typically dominate different zones as waves from a deeper region reach a breaking zone, and then waves with new characteristics regenerate and move further shoreward. Some typical zone transitions include:

- The deeper open Gulf of Mexico to the Continental Shelf;
- The Continental Shelf to the nearshore zone of barrier islands and headlands;
- Open water in larger sounds, bays, lakes, and channels to their nearshore zones; and
- Smaller bays, lakes, channels, and submerged coastal wetlands to the nearshore (foreshore) of natural and artificial embankments.

Hurricane waves are irregular—meaning the height (H), period (T), and direction of individual waves vary within a wave field. Wave heights do not vary in a normal distribution but are instead typically characterized by the skewed (i.e. asymmetrical) Rayleigh distribution as shown in Figure 5.4. In this distribution two important conditions are *the significant wave* (H_s, the average of the upper one-third waves), and *the 1% wave* (the wave that occurs once out of every 100 waves on average).[1] These statistical conditions within a wave field change during the course of a storm as SWL rises and falls and as winds rise/fall and shift direction. Over the course of a two-hour SWL peak a wave field with an average period (T_{avg})[2] of 8 seconds will produce a total 900 waves. If the wave field contains a representative number of the various waves, nine 1% waves will occur. However, the probability of any single two-hour wave field containing nine (or more) 1% waves is actually 54%.

Obtaining accurate wave spectrum data requires a very high frequency capture rate platform- or buoy-mounted gauge. Compared to SWL data there is a significant dearth of hurricane coastal wave data in all zones. The peak elevation of SWL-plus-wave for inundated areas can sometimes be gleaned from HWMs along open exposed walls or from floating debris left in trees or along embankments.

---

[1] $H_{avg} = 0.625H_s \approx 5/8\ H_s$; $H_P = .705H_s\ (-\ln P)^{1/2}$, where P is the Percentile, e.g., $H_{1\%} = 1.52H_s$ and $H_{0.1\%} = 1.9H_s$

[2] T_{avg} and T_p refer to the wave periods (1/frequency) containing the average and peak wave energy.

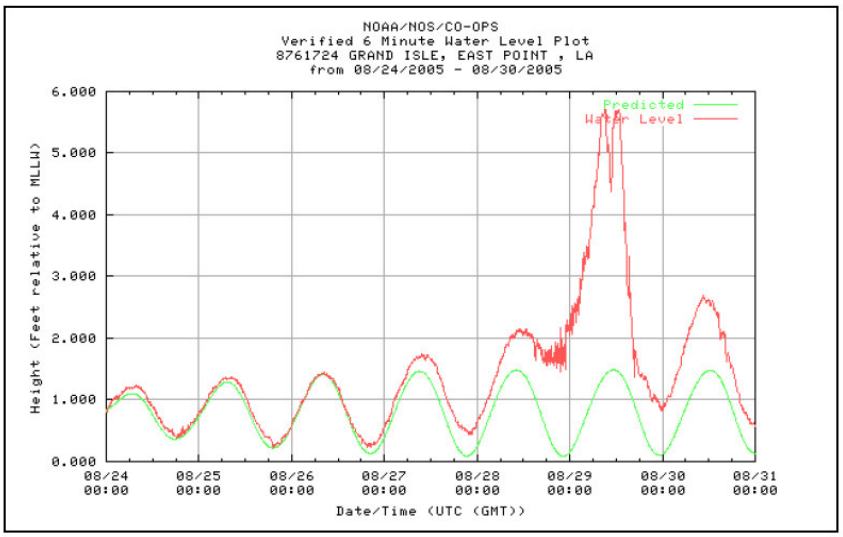

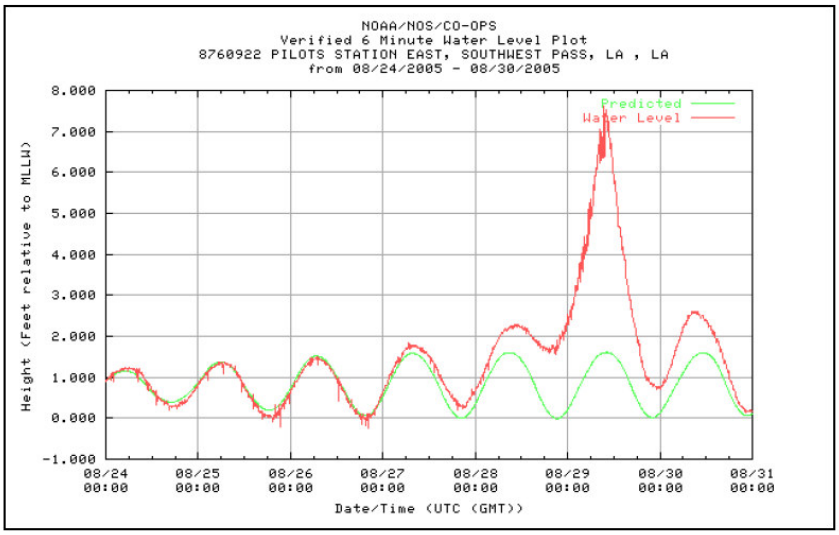

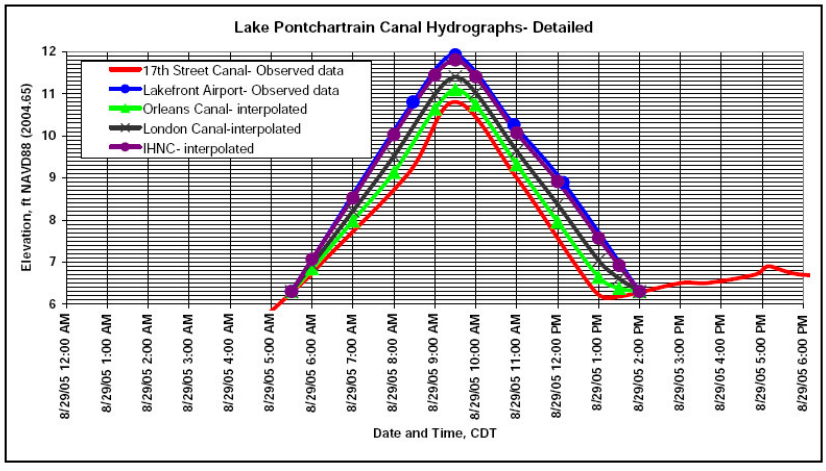

Figure 5.3. Hurricane Katrina Surge Hydrographs
IPET 2006

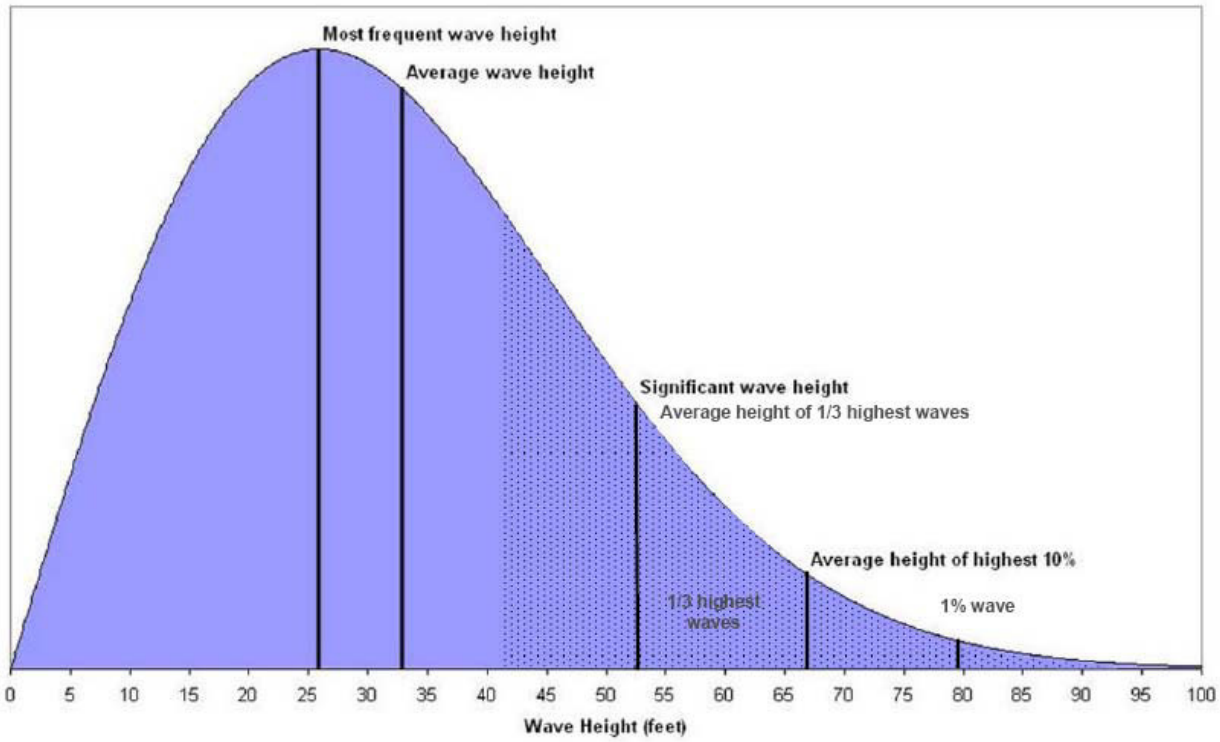

Figure 5.4. Rayleigh Distribution for Hurricane Ivan Waves at Buoy 42040
NOAA, http://www.vos.noaa.gov/MWL/aug_05/nws.shtml

5.2. Surge Dynamics

The surge dome shape changes as it approaches landfall, depending on the individual hurricane core intensity and size, wind field, dynamics, forward speed, and track and specific interactions with the local coast. The spatially varying surge SWL above LMMSL at any snapshot in time is termed the *setup* (η). Over expansive open water and inundated land with flat bathymetry the *setup slope* can be less than half a foot per mile. But with declining depth, the wind stress raises the dome height and the setup slope. When the surge encounters elevated obstructions, the dome is also squeezed, further steepening the setup slope, sometimes reaching two feet per mile. Variations in landscape compression of surge domes are analogous to the different effects of spilling a large drum of water in the middle of a room, versus close to a wall, or near a corner.

The varying magnitude and direction of winds contained in a hurricane wind field produce widely varying surge effects. The rise and fall of surge is fastest with the landfall of the dome peak, typically just to the right of the hurricane center. At this location the SWL is capable of rising several feet per hour. To the left of landfalling dome the offshore winds can produce a SWL s*etdown* below LMMSL (negative η). Secondary eyewalls and wind banding can cause irregularities in regional setup/setdown.

Landfalling surge domes exhibit elongation, turning, and fingering as they are forced over and around the coastline and its natural and artificial barriers. Figure 5.5 depicts surge dynamics for Hurricane Katrina in a series of plan views based on a computer simulation (USACE 2008). Peak SWLs actually reached above 18 ft (NAVD88-2004.65) in eastern St. Bernard Parish (Reggio) and in excess of 13 ft along Lake Pontchartrain in Little Woods in eastern Orleans Parish (URS 2006).

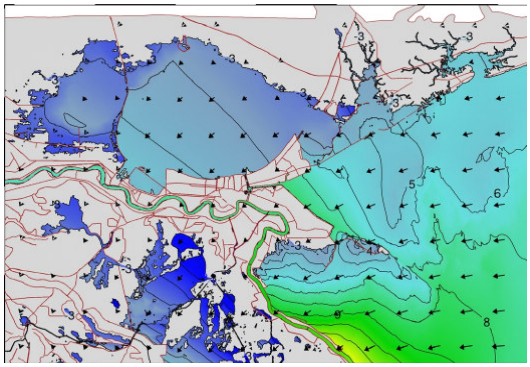

2 am CDT August 29, 2005

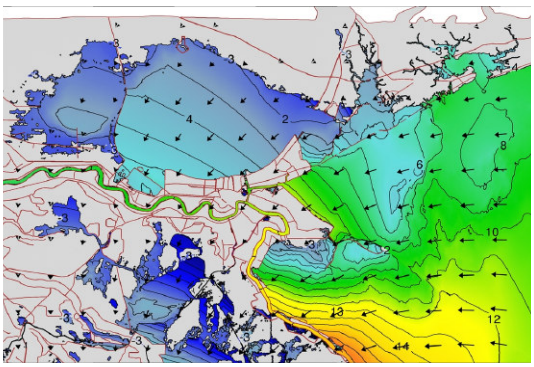

5 am CDT August 29, 2005

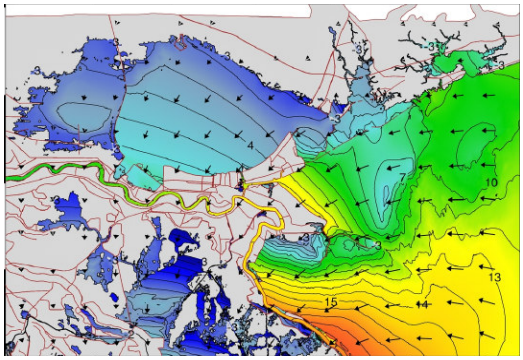

6 am CDT August 29, 2005

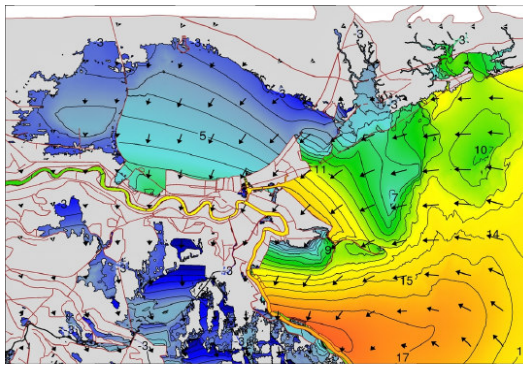

7 am CDT August 29, 2005

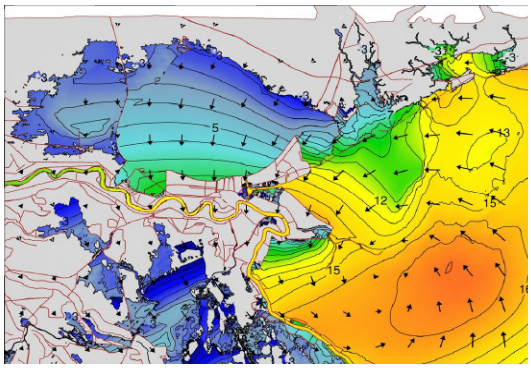

8 am CDT August 29, 2005

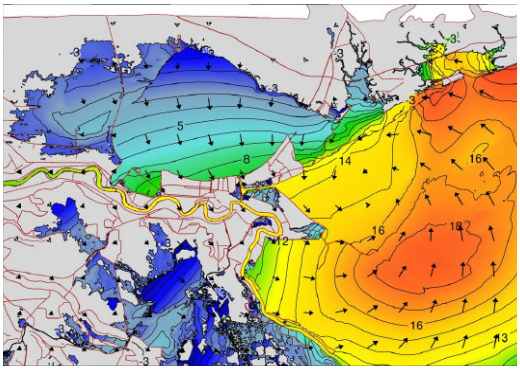

9 am CDT August 29, 2005

Figure 5.5. Hurricane Katrina Surge Dynamics
(approximated using computer simulation)
USACE 2008

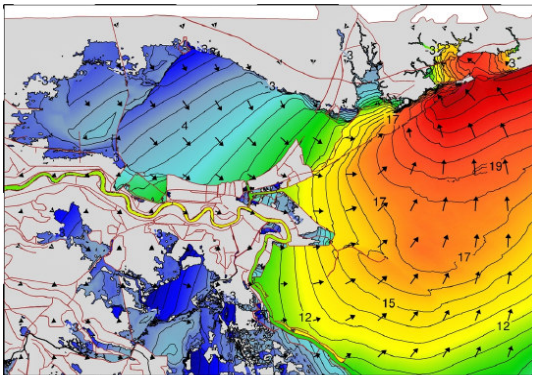

10 am CDT August 29, 2005

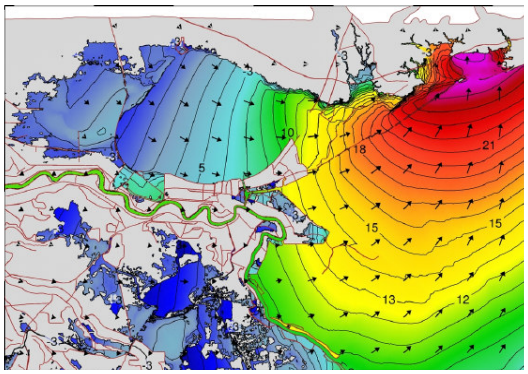

11 am CDT August 29, 2005

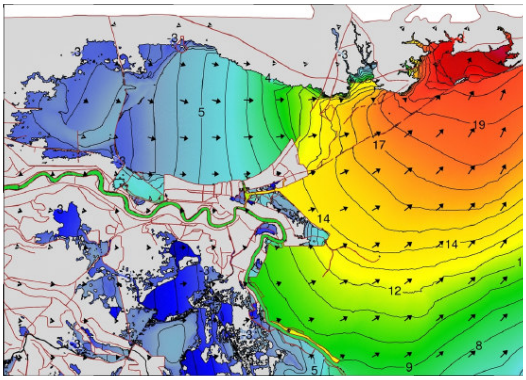

12 pm CDT August 29, 2005

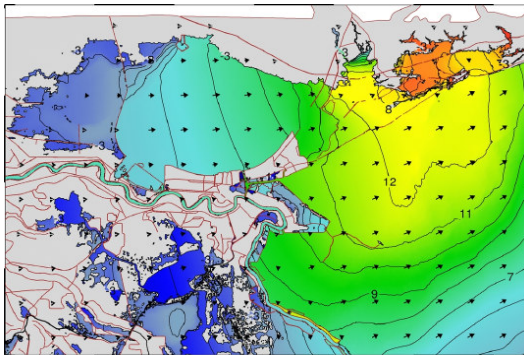

3 pm CDT August 29, 2005

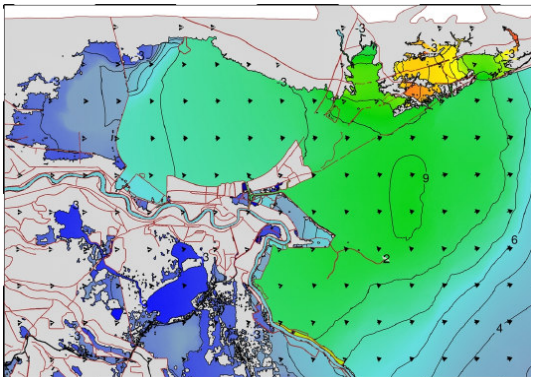

6 pm CDT August 29, 2005

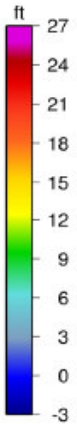

Surge Elevation (NAVD88)

Figure 5.5. (continued) Hurricane Katrina Surge Dynamics
(approximated using computer simulation)
USACE 2008

Section 6. Surge Physics

6.1. Surge SWL Physics

The particular surge dynamics of an individual hurricane are governed by fundamental physical hydrodynamic laws (see Resio and Westerink 2008). The total surge domain at any point in time can be considered as a vast collection of individual vertical columns of water (much like the way a flat image is composed of pixels) The treatment of a water body as a set of vertical columns allows for a two-dimensional (2D, i.e., *x* and *y*) analysis of surge SWL physics in which all exchanges, forces, velocities, and acceleration are considered only in the lateral direction, with a depth averaged value at each column.[1] These physical interactions are governed by three basic laws:

1. Conservation of mass dictates that 1) over the entire domain and duration of the event the total volume of water must remain equal to the initial volume; [2] and 2) over any increment of time the change in water depth (i.e., SWL or η) within each individual water column must equal the amount of water exchanged with the surrounding columns or the atmosphere.
2. Conservation of momentum requires that the net lateral forces acting on each individual column at any *instant* of time must be balanced by the sum of the column's two inertial conditions—the column average lateral acceleration (i.e., rate of change in lateral velocity) with respect to time and space—multiplied by the column's mass (proportional to water depth). If the net forces zero out, then the column has no acceleration. Over any *increment* of time, a change in the net forces on an individual column must equal a change in the mass times acceleration—either the mass, the acceleration, or both.
3. The conservation of energy requires—as with a pendulum—that the kinetic energy of the oncoming surge wave prior to landfall must be translated into to a combination of a) increases in surge potential energy (i.e., rising onshore inundation; b) outgoing wave energy; and c) energy spent on friction and erosion. In equation forms momentum and energy conservation for surge closely mirror each other so reference is typically made simply to the momentum, or force, equation.

The 2D momentum conservation law encompasses ten forces acting on each column. The magnitude and direction of forces are defined in terms of input variables and empirical coefficients (parameters).[3] The first three of the ten lateral forces are familiar from basic open channel flow dynamics and include:

1. *Water pressure,*[4] which is proportional to the difference in depth between adjacent columns.

---

[1] A rigorous analysis decomposes the water body into three-dimensional blocks and considers physical interactions in the vertical as well. The 2D physics are then derived from the 3D on the basis of simplifying assumptions. All applied (as opposed to research) studies currently employ a 2D treatment of hurricane surge physics.

[2] The domain boundary is set far enough away that it is assumed to be unaffected by the hurricane.

[3] Empirical coefficients are obtained from scientific/engineering literature based on experiments or analysis of event data. Input variables are either those generally taken as constants, such as the acceleration of gravity and the specific gravity and viscosity of air and seawater, or those based on measurements or assumptions associated with a particular scenario (e.g., wind conditions). Variables to be solved include the water depth and velocity.

[4] Some forces are commonly expressed in terms of pressure and stress, which are simply forces per unit area (normal and tangential, respectively) to the line of force.

2. *The lateral component of the bed reaction force*—proportional to the bathymetric slope and gravity (and sometimes referred to as a gravity component)—in the direction of downhill. The first two forces can be combined, into a single force proportional t0 the change in η.

3. *Friction,* a drag force (or shear stress) which is exerted laterally in opposition to moving water by bottom roughness and obstructions. Friction is proportional to the water column lateral *velocity squared (V^2)* and an empirical *friction coefficient*. Hydraulic analysis frequently uses a simplified one-dimensional (i.e., channel) equation ignoring water pressure (the Manning's Equation) which estimates a setdown (call a headloss in hydraulics) in the direction of flow proportional to the V^2, the *friction coefficient squared (n^2)*, and the flow path *length*, and inversely proportional to the *depth raised to the four-thirds power*.[5] The combination of the last three terms is called the *conveyance*. The Manning's *n* coefficient depends on the type, density, and submergence of vegetation and other obstructions.

Extensive research on riverine flooding over vegetated floodplains has verified the use of momentum balances involving water pressure, gravity, and friction and provides the basis for Manning's *n* values. However, appropriate Manning's *n* values for surge events are still a subject of ongoing research both in the open ocean, Continental Shelf (Kennedy et al 2011), and overland. For example, as submergence increases the Manning's *n* value for flow over a marsh can drop by up to an order of magnitude. This difference in the friction coefficient can have a significant effect because headloss is proportional to n^2.

A fourth lateral force is added when channel hydraulics are considered in 2D:

4. *Turbulent stress*, which accounts for horizontal eddies (swirls) in the flows that laterally diffuse momentum. This force describes momentum spreading between adjacent columns that is not captured by the other terms depicting momentum transfer at larger scales. The rate of spreading can be considered proportional to an eddy viscosity coefficient and the local velocity gradient. The eddy viscosity coefficient, in turn, can be considered a function of the column width and local velocity gradient condition (after Smagorinsky).

Empirical coefficients for quantifying the influence of horizontal turbulence in momentum balances are not well defined, especially for surge events, and research is needed to improve methods of representing turbulent stress.

Two more lateral forces considered in coastal hydrodynamics are:

5. *Astronomical tides*, which are created by gravitational effects of the sun and moon. The magnitude and direction (onshore versus offshore) of tides are well established and can be readily interpolated to each column.

6. *Coriolis force*, which is caused by the earth's rotation and deflects moving bodies of water to the right in the northern hemisphere in proportion to the latitude

During hurricanes and other storms three additional lateral forces act on the coastal water column:

7. *Atmospheric pressure*, which produces a direct rise of about 4 inches in water level for every 10 mb drop in overlying air pressure with respect to the far field ambient pressure. However, the hurricane CPD primarily influences surge not through the direct rise but by inducing a wind vortex (see Part I).

[5] For narrow channel flow the hydraulic radius is used in place of depth.

8. *Wind drag*, which is a shear stress that moves the water column in the direction of the circulating hurricane winds. Wind drag is a function of the *wind* V^2 [6] and an empirical *air-sea drag coefficient*. The air-sea drag coefficient, in turn, depends on the roughness of the water surface (i.e., wave field). Adequate characterization of hurricane air-sea drag coefficients has been hampered by lack of observations for wave fields and surge velocity. (Powell et al 2003). In onshore areas, wind drag is reduced by sheltering from trees and buildings. In a simple equation wind driven setup is proportional to wind drag and *fetch* (the wind path length over open water) and, importantly, inversely proportional to water depth. The wind drag is responsible for most of the surge SWL rise (Kurian 2009).

   All other factors being equal, maximum storm surge SWL is generally proportional to the wind V_{max}^2—which in turn is generally proportional to hurricane core CPD, (Resio et al 2007). (Part I describes several proposed alternatives to the Saffir-Simpson Scale based on V_{max}^2. For two hurricane storms with equivalent V_{max}^2 but different R_{max}, the larger core storm will exert its wind drag over a larger area. Figure 6.1 illustrates the combined role of core intensity (as measured by CPD) and R_{max} in producing a peak surge for a generic, straight, shallow planar shoreline (Irish et al 2008), with all other hurricane attributes held equal.

9. *Radiation stress* exerted by waves. A dramatic spatial variation in wave heights—such as from nearshore wave shoaling and breaking (see next section)—creates a steep spatial gradient in the radiation stress. The radiation stress gradient is balanced by a corresponding setdown in SWL at the wave breaking point and a setup at the shoreline. These are referred to as *wave setdown and setup* (see Figure 6.2) and contribute to η. The wave setdown at breaking is on the order of 5 percent of the breaking significant wave height. The wave setup is up to 20 percent of the breaking significant wave height. For a breaking significant wave height equivalent to 50% of the depth, the setdown and setup are 2.5% and 10% of the breaking depth. Depending on the local breaking depth at peak surge, the wave setup can contribute about 10 to 30 percent of η along the open coast shoreline (Resio et al 2007). Shoreline geometry and bathymetry can create notable long shore gradients in wave setup, thereby inducing long shore currents.

The 2D physics encompassing these nine forces are “barotropic” as opposed to “baroclinic,” which must add addition equations to describe lateral variations in water temperature and salinity, and thus, density. Researchers are studying three dimensional (3D) surge physics, incorporating vertical density variations as well as a tenth force, (see Resio and Westerink 2008, Dresback et al 2010, Weaver and Luettich 2010, Weisberg and Zheng 2008):

10. *Buoyancy,* which drives relative movement of lighter (warmer, fresher) and heavier (colder, saltier) layers—particularly near coastal passes with high temperature and salinity gradients.

The 3D analysis can be *hydrostatic*, addressing only depth variations in 2D forces and acceleration, or fully 3D, considering actual vertical components of forces and acceleration.

[6] See Section 1, Footnote 1 for a discussion of hurricane wind averaging periods, e.g., 30-, 10-, 1-minute, and 3-s gusts.

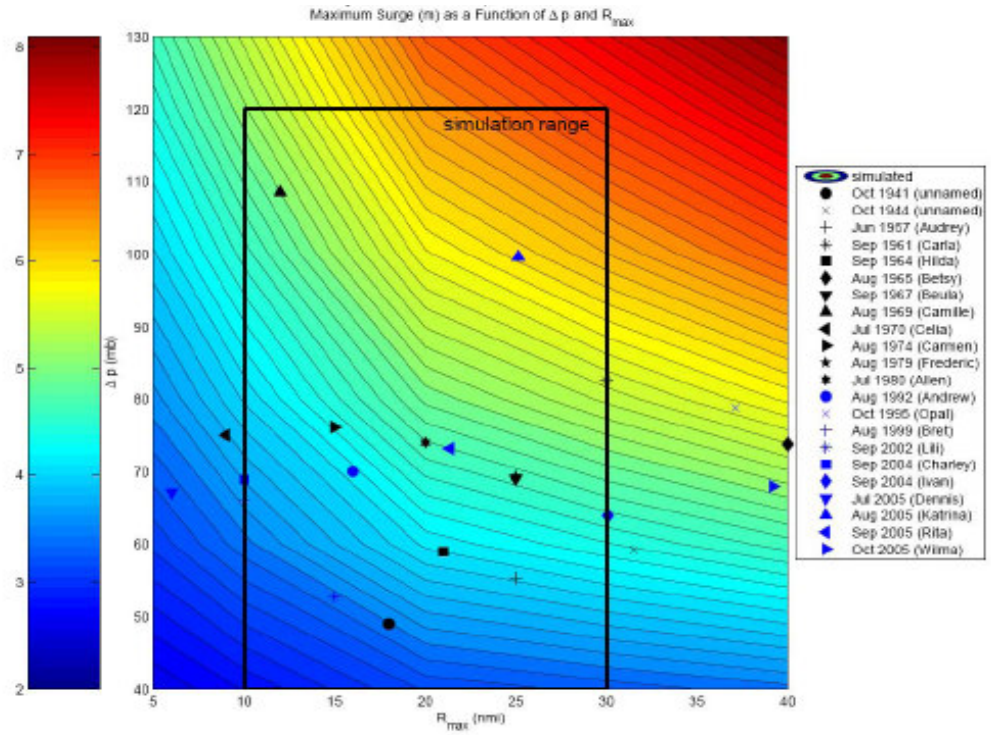

Figure 6.1. Combined Influence of Hurricane Core Intensity and Size on Surge
Irish et al 2008

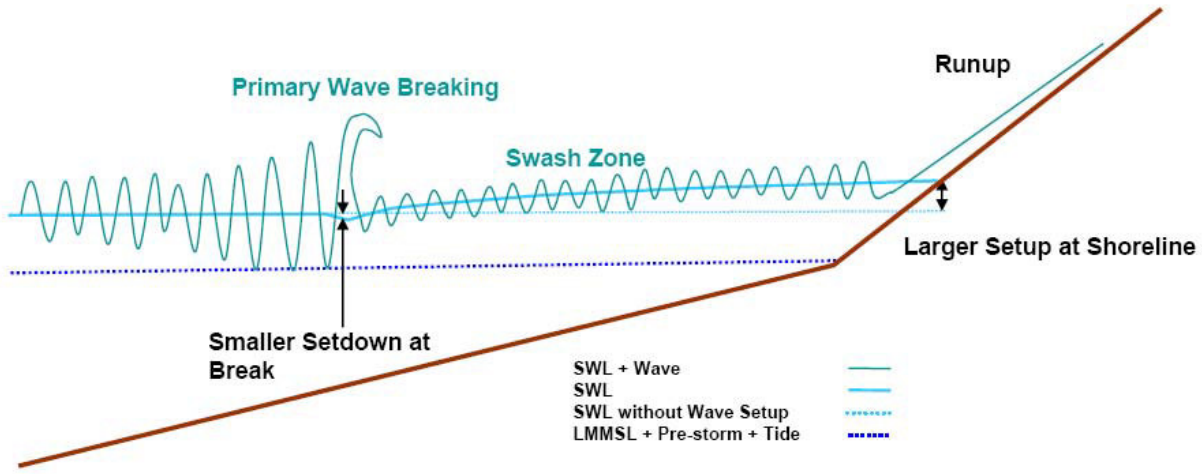

Figure 6.2. Nearshore Wave Setdown and Setup Influence on SWL
(not to scale)

Figures 6.3.a. through d. present a simplified schematic of 2D surge physics, including the shoreward wind drag, seaward bed reaction, and overland friction resistance. With advancing overland surge (Figure 6.3.b.) the landward forces (primarily wind drag and water pressure) are countered by friction and bed reaction. As the surge approaches its inland peak (Figure 6.3.c. or d.) the friction force declines (due to the reduced velocity near peak) and the landward wind drag is balanced by seaward water pressure and gravity. As illustrated in Figures 6.3.c. and d., coastal surge barriers compress the advancing surge and adjust the balance, with landward conveyance obstruction coming at the expense of higher flood-side setup.[7] This aspect of surge physics is clearly shown in Figure 5.5, which shows the setup induced by the southeast Louisiana regional hurricane protection system at various times during Hurricane Katrina.

6.2. Wave Physics

Estimating the potential contribution of waves to hurricane hazards—both to SWL setup as noted above and through the waves themselves—requires understanding wave physics. Eight important wave physical processes include (see Dean and Dalrymple 1991):

1. Open ocean wave generation, which depends on wind velocity and fetch and provides the basic deep water irregular wave field conditions (H_s, T_p) prior to waves entering the Continental Shelf zone.
2. Wave shoaling, in which wave heights increase and wavelengths shorten due to reduced depth. As Hurricane Ivan (2004) crossed from the deep Gulf of Mexico onto the Continental Shelf (east of the Mississippi River delta) significant wave and maximum wave heights were estimated to exceed 60 and 120 feet, respectively (Wang et al 2005).
3. Friction, (e.g., muddy bottoms, wetland vegetation for inundated coasts) which can reduce wave heights through energy dissipation (Anderson et al 2011)
4. Wave breaking at limiting depths. As depth declines, waves reach a point at which they break. H_s:depth ratios have been proposed at 0.4 to 0.7 depending on local conditions (USACE 2010). Nearshore wave data collected along the Texas coast during Hurricane Ike (2008) showed that breaking H_s was about half the SWL depth (Kennedy et al 2010). For overland waves in inundated vegetated terrain, a ratio at the lower end of the range would be expected, but research for such conditions is very limited. Research is also limited on characterizing wave height distributions in various post-break environments.
5. Wave regeneration in interior bays, lakes, and large channels.
6. Wave field transformations (H_s, T_p) due to interactions with surge currents.
7. Wave field refraction (bending due to incident angle interaction with the general bathymetry), diffraction (bending around obstacles and after passage through openings, such as barrier islands, passes, and headland points), and reflection. These processes can cause wave energy to become focused at particular locations.

[7] A detailed study of surge dynamics in southeast Louisiana absent the current regional hurricane protection system has not been undertaken.

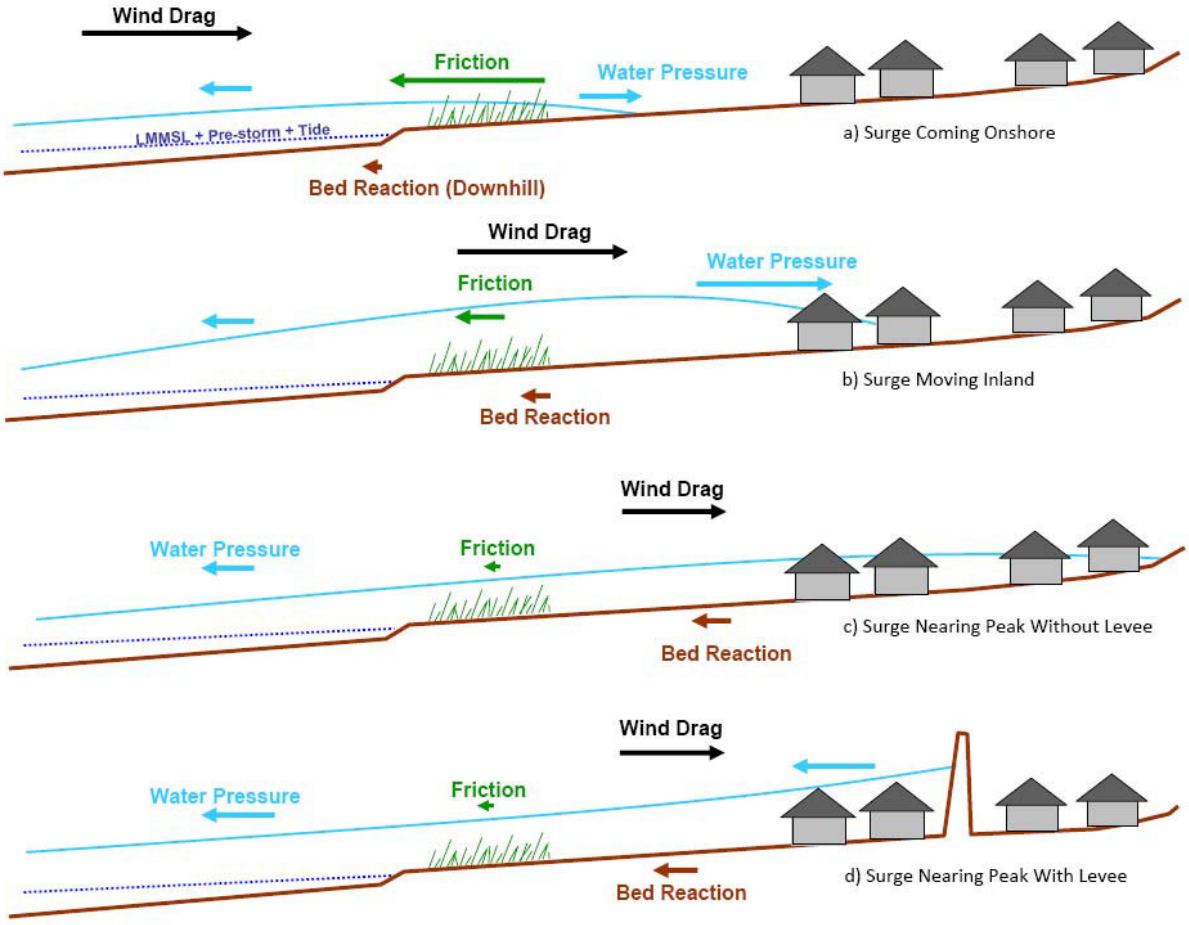

Figure 6.3. Simplified Schematic of Surge Physics
(not to scale)

8. Wave runup, which occurs when a broken wave rolls up the shore face. The wave momentum pushes water up the slope to a height greater than that of the nearshore pre-break wave (see Figure 6.2). The runup height depends on the pre-break wave height, wave steepness, shore slope, and slope roughness. The runup height of the maximum wave is referred to as the maximum runup.

Data depicting wave processes in shallow interior water bodies and over land during hurricanes is very sparse. Available empirical equations describing these processes rely primarily on idealized laboratory experiments or observations for nearshore conditions less dynamic and less extreme than hurricanes. In addition, the short time over which peak surge conditions occur may reduces the applicability of empirical generalizations derived for near-steady wave fields. Thus, extensive research on hurricane wave conditions is required to improve confidence in their mathematical representation.

Section 7. Surge and Coastal Landscape Interactions

Surge dynamics result from a hurricane's attributes (core intensity, size, wind field distribution, forward speed, and track) setting a quantity of Gulf of Mexico water in motion, and the interaction of that large moving mass of water with the landfall area coastal landscape features, as governed by the physics of mass and momentum conservation. Coastal landscape features interact with three specific aspects of the regional and local surge physics: wind setup, surge conveyance, and wave processes (see Interaction of Hurricane and Coastal Landscape Features: A Literature Review, Suhayda and Jacobsen 2007). Coastal landscape features occur at a range of scales—regional to local--and often influence two, or even all three, aspects of surge physics.

7.1. Features Influencing Wind Setup

Coastal features influence wind setup through sheltering (reducing wind) or by affecting fetch or water depth. Such features are present at a wide range of spatial scales, with the largest features having the greatest potential impact. An important large-scale, coastline geomorphologic feature influencing wind setup is the presence of an extensive, shallow Continental Shelf, such as in the northeastern Gulf of Mexico. The counterclockwise winds of hurricanes approaching Mississippi River Delta will exert a westward drag across the lengthy fetch of the relatively shallow shelf fronting the Mississippi/Alabama/Florida Panhandle, shown in Figure 7.1. The combination of an intense westward wind drag, long fetch, and shallow depth creates the potential for significant wind setup along the eastern flank of the Delta. The wind setup is enhanced in those cyclones that enter the eastern Gulf of Mexico and traverse westward, e.g., Hurricanes Betsy (1965) and Katrina (2005). Even hurricanes that make landfall in southwest Louisiana or eastern Texas can drive significant surge into the eastern Delta and Lake Pontchartrain if they exert a sustained and heavy wind drag along this portion of the Continental Shelf. e.g., Hurricanes Rita (2005) and Ike (2008).

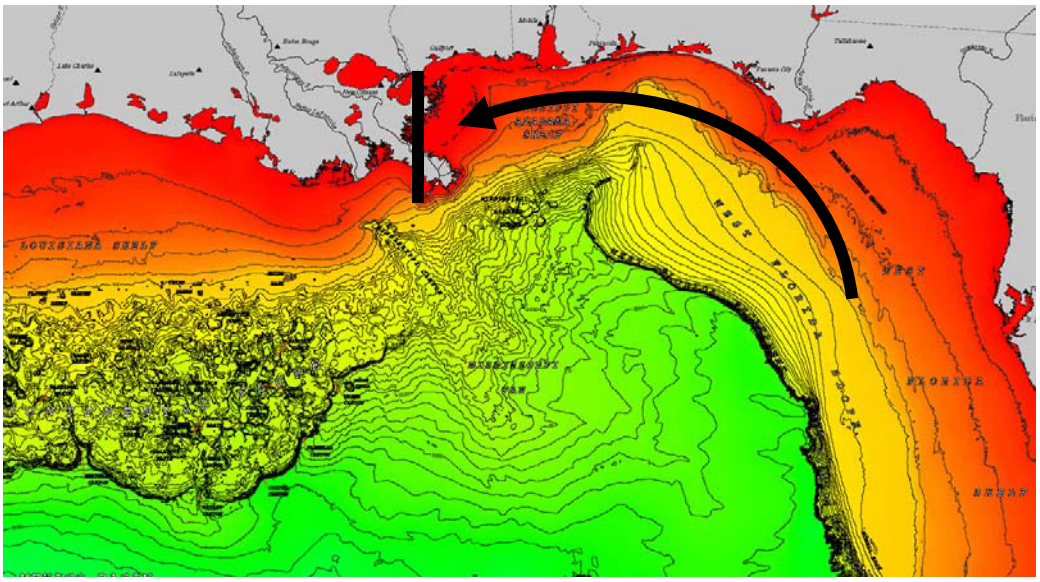

Figure 7.1. Bathymetry of the Gulf of Mexico Continental Shelf
http://ngdc.noaa.gov/mgg/ibcca/images/1234.jpg

In 2010 Fitzpatrick et al evaluated surge differences for a hypothetical coastline—with a range of shelf bathymetric slopes over a perpendicular offshore distance of 200 miles—for a variety of hurricanes. As illustrated in Figure 7.2, they found that shallow shelves can produce surge more than twice as high as deep shelves, consistent with wind setup physics. The authors further evaluated the role of shelf bathymetry with a combined hurricane size-intensity factor ($IKE^{1/2} * V_{max}$, see Part I) on surge. Figure 7.3 indicates that surge approximates a linear function of the size-intensity factor at various bathymetries.

It is important to note that the influence of shelf bathymetry on surge is different than for a tsunami. For hurricane surge, a long shallow shelf amplifies the wind setup which results from wind drag acting across many tens of miles of water surface. A tsunami wave is generated at a particular offshore location and propagates toward the coast. Against a steeper coastal bathymetry the tsunami compresses more rapidly and produces a higher SWL; whereas a shallow shelf causes the tsunami to dissipate energy, producing a lower SWL over.

Large scale coastal protrusions like the Mississippi River Delta also affect hurricane winds. As storms approach landfall near those protrusions, winds rotating into the left front quadrant experience increase land drag, which can lead to storm infilling and decay (see Part I). Similarly, expansive forested coastal landscapes can produce more infilling than open marsh. The core intensity of major hurricanes are more likely to be affected by land-wind interaction than less powerful storms.

Two significant types of local scale wind setup features include:

1. Barrier islands and long headland spits, ridges, and cheniers (e.g., Grand Isle, Caminda Headland, Bayou La Loutre, Chenier Caminda). These features, particularly when densely forested, can reduce wind drag in leeward sounds, bays, lakes, and inundated areas.

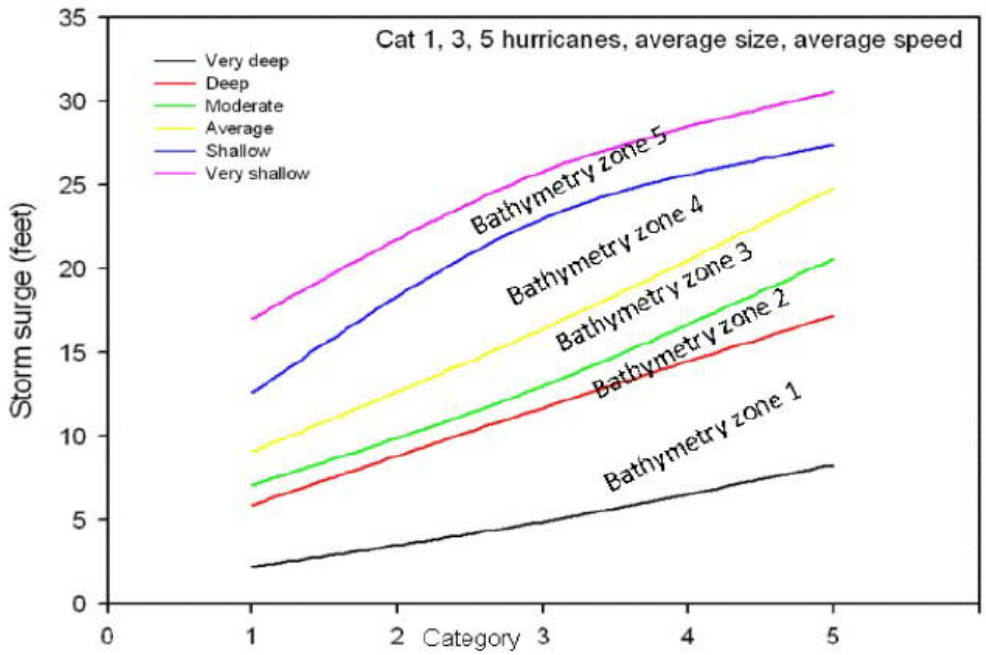

Figure 7.2. Influence of Shelf Bathymetry on Surge for Hurricanes by Category
Fitzpatrick et al 2010

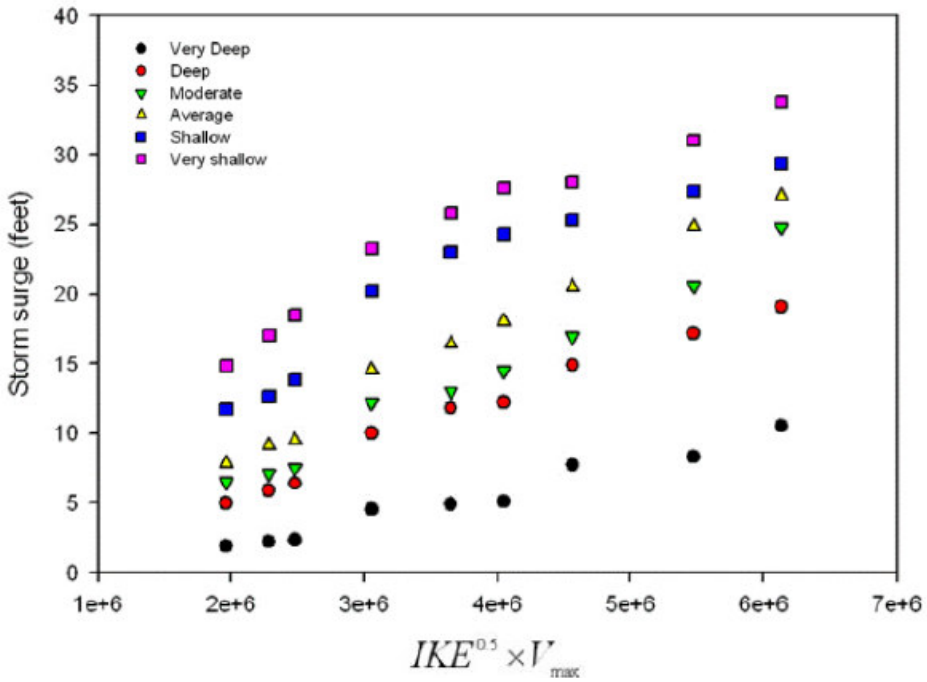

Figure 7.3. Influence of Shelf Bathymetry on Surge for Hurricanes by IKE-Vmax Factor
Fitzpatrick et al 2010

2. Large, shallow sounds, bays, and lakes. Hurricane winds readily "fill and tilt" Lakes Borgne, Pontchartrain, and Maurepas. Hurricane Katrina first filled Lake Pontchartrain, raising SWL to about 5 ft, and then exerted strong northerly winds over the lake as it passed just to the east, tilting water up onto the south shore to elevations over 12 ft. In 1979 Crawford employed the newly developed Sea, Lake, and Overland Surge from Hurricanes (SLOSH) model to study the varied impacts of hurricane winds acting across Lake Pontchartrain based on track, see Figure 7.4.

The effect of local features depends on the particular wind field strength, duration, and orientation.

7.2. Features Influencing Conveyance

Conveyance features—through variations in the flow length, depth, and friction coefficient (Manning's *n*)—divert surge movement. The exponents of the conveyance headloss variables—length, depth$^{4/3}$, and Manning's n^2—influence their relative importance. Five important categories of conveyance features are illustrated in Figure 7.5, and include:

1. Flood protection and other hydraulic control structures. These structures are purposefully designed to obstruct and divert the movement of surge. In reducing flood depths on the protected side they necessarily increase flood side setup. Regional examples of flood protection and other hydraulic control structures include:

   - HSDRRS levees and floodwalls;
   - Navigation locks. e.g., IHNC, Algiers, Harvey;
   - Floodgates, e.g., Gulf Intracoastal Waterway (GIWW) and Seabrook; and
   - Channel weirs/closures, e.g., Mississippi River Gulf Outlet (MRGO) at Bayou La Loutre.

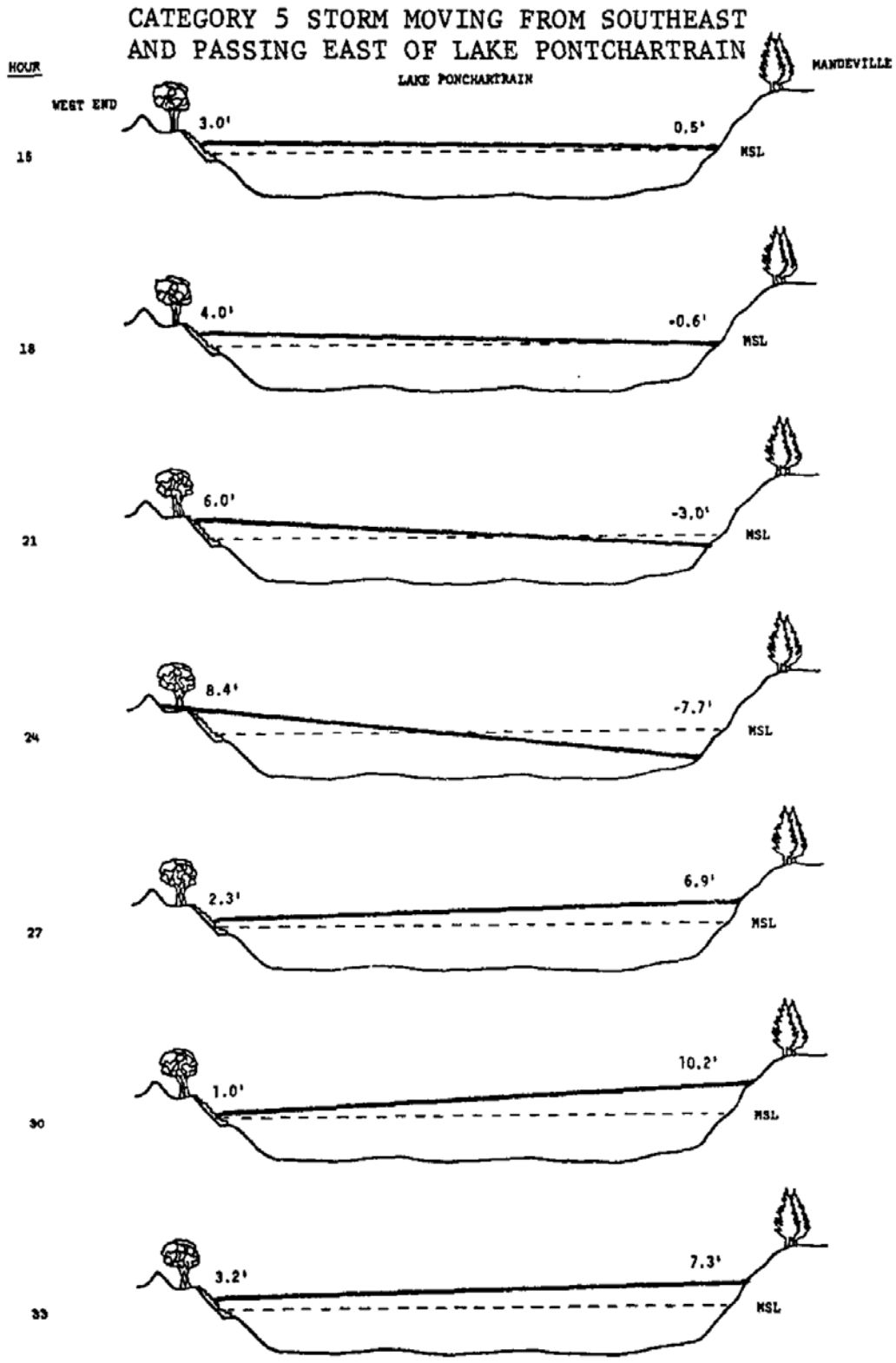

Figure 7.4. Tilting of Lake Pontchartrain in Response to Strong Hurricane
Crawford 1979

a. Hurricane Protection Levee: Plaquemines Parish Levee at Braithwaite LA, Hurricane Gustav

b. Hurricane Protection Floodwall: Industrial Canal Floodwall, Hurricane Gustav

Figure 7.5. Photographs of Coastal Conveyance Features

c. Hydraulic Structure: Mississippi River Gulf Outlet Closure Structure

d. Railroad Embankment: CSX Railroad Crossing, New Orleans East
(U.S. Army Corps of Engineers photo)

Figure 7.5 (continued) Photographs of Coastal Conveyance Features

e. Barrier Islands: Chandeleur Islands

f. Coastal Headland: Caminada Headland

Figure 7.5. (continued) Photographs of Coastal Conveyance Features

g. Coastal Ridge: Ridge Along Bayou Terre aux Boeufs

h. Coastal Pass: Chef Menteur Pass

Figure 7.5. (continued) Photographs of Coastal Conveyance Features

i. Coastal Forest: Maurepas Swamp

j. Coastal Marsh: Delacroix Marsh

Figure 7.5. (continued) Photographs of Coastal Conveyance Features

k. Coastal Channel: Mississippi River Gulf Outlet Reach 2
looking east at Bayou La Loutre

l. Interior Channel: Junction of Mississippi River Gulf Outlet Reach 2 (Left) and Gulf Intracoastal Waterway (Foreground) and Reach 1 (Extending under the Paris Road Bridge), "The Funnel"

Figure 7.5. (continued) Photographs of Coastal Conveyance Features

2. Other man-made embankments. These features consist primarily of built-up earthen subgrades for roads, railroads, and bridge approaches and are potentially important to surge conveyance when they transect low-lying coastal marshes and swamps. Examples include:

   - The CSX and Norfolk-Southern railroad embankments in New Orleans East;
   - The Canadian Northern railroad embankment along Lake Pontchartrain in St. Charles Parish;
   - US Highway 90 in New Orleans East; and
   - Louisiana Highways 46 and 300 in eastern St. Bernard and Plaquemines Parishes

3. Natural topographic barriers. Significant natural topographic barriers include:

   - Barrier islands, e.g., Chandeleur and Breton Islands;
   - Headland dune complexes, e.g., Caminada Headland;
   - Cheniers, e.g., Chenier Caminada; and
   - Inland ridges and remnant distributary natural levees, e.g., Bayou LaLoutre Ridge in St. Bernard Parish. Extended ridges, known as *land-bridges*, particularly those that are accompanied by man-made roads or railroad embankments, are important conveyance obstructions. Examples include the New Orleans East and Manchac land-bridges.

   As with flood protection structures, road/railroad embankments and natural topographic barriers can obstruct and divert the movement of surge. The degree of conveyance control exerted by these features depends on:

   - Barrier Length. Given the size of a surge long wave, short features have little effect on surge events;
   - Elevation. To be effective as a surge barrier the feature cannot be submerged;
   - Gaps. Numerous or large openings substantially reduce the effect on surge;
   - Erodibility. Features made of fine sands, silts, or noncohesive organic material may not withstand surge hydrostatic, wave, and overtopping forces; and
   - Armoring. Man-made embankments that are hardened (e.g., asphalt and concrete roads, rip rap armored slopes) and natural ridges that are well vegetated are more likely to withstand erosion.

4. Land cover. Lengthy flow paths with high friction can absorb significant surge energy, ultimately reducing the inland setup (Loder 2008). The Manning's *n* value for densely vegetated wetlands (e.g., forested swamps with heavy underbrush) can be up to five times greater than for broken marsh and up to ten times greater than for open water.

5. Preferential conveyance pathways. These include:

   - Passes and inlets, e.g., Caminada, Barataria, Rigolets and Chet Menteur Passes;
   - Large coastal/estuarine waterbodies, such as sounds, (e.g., Breton, Chandeleur, and Mississippi), bays (e.g., Barataria, Terrebonne), and lakes (e.g., Borgne, Pontchartrain, and Maurepas);
   - Coastal channels, e.g., the Mississippi River below Venice and the MRGO Reach 2 (see discussion below on impact relative to surge conditions);
   - Interior channels, e.g., the Mississippi River above Venice, MRGO Reach 1.

A very important large-scale conveyance feature in southeast Louisiana is the eastbank Mississippi River Delta—comprised of the remnant marshes and ridges in St. Bernard delta (e.g., Biloxi and Delacroix marsh), Plaquemines delta, and Beliz delta. As shown in Figure 7.1, hurricanes that create massive westerly wind setup along the northeastern Continental Shelf (see above) squeeze surge against the eastern flank of the southward extending Delta. Such surges are further trapped and compressed by the extension of the Biloxi Marsh and New Orleans East land-bridges across the mouths of Lakes Borgne and Pontchartrain. The overall effect is that surge is pushed into a "corner"—much like a drum of water spilled into the corner of a room—with the communities of Waveland and Bay St. Louis at the vertex. In addition to this large-scale corner, there are local corners including the junction of HSDRRS structures along the MRGO and GIWW at the IHNC Surge Barrier, and the junction of the HSDRRS levee with the Mississippi River Levee at Caernarvon.

7.3. Features Influencing Wave Processes

Wave features influence one or more of the seven processes described above and can be located in any of the various zones. The most important class of wave features are those that affect breaking and regeneration. Figure 7.6 provides examples of wave features. Seven important categories include:

1. Offshore expansive shoals, reefs, mud lumps, and submerging barrier islands, which can transform and possibly break the large ocean waves, (e.g., Ship Shoal, Chandeleur Islands);
2. Barrier islands and long headland spits and ridges (e.g., Grand Isle, Caminada Headland, Bayou La Loutre Ridge) which reduce surface winds and leeward wave regeneration.
3. Non-flood protection embankments and natural topographic barriers, which act as inland breakwaters (e.g., roads, railroads, ridges).
4. Large shallow coastal/estuarine water bodies over which winds can generate substantial waves (e.g., Lakes Borgne, Pontchartrain, and Maurepas).
5. Land cover and water bottom. The same friction sources that reduce conveyance can also dampen waves, enhance wave breaking, and reduce wave regeneration when they are not overly submerged, e.g., forest swamps with heavy underbrush (Loder 2008). In addition, the presence of a thick layer of viscous mud can transform waves.
6. Breakwaters (continuous or segmented). They are typically located in the nearshore (e.g., Fourchon, and Grand Isle) or foreshore (e.g., the south shore of Lake Pontchartrain).
7. Shoreline erosion stabilization. These features are designed to mitigate erosion by direct wave attack and long shore currents, and manage the transport and deposition of sediments. Coastal sediment controls include jetties, groins, and foreshore armoring. Major regional jetties include those at the mouth of the MRGO and Barataria, Caminada, and Fourchon Passes. Examples of shore armoring include foreshore rip rap (e.g., Lakes Borgne, Pontchartrain, and numerous other water bodies), concrete stepped seawalls (e.g., Lakefront Park in New Orleans), and sheet pile bulkheads (primarily along the banks of developed properties). These features reinforce the shoreline and hold the slope and foreshore in place. When the shoreline become submerged armoring can play a role in wave breaking, particularly if it is elevated above the shore.

These features also affect local hurricane waves through wave refraction, diffraction, and reflection, as well as interactions with surge currents. Local coastal features can produce complex variations in wave heights (up to several feet) and wave setup (greater than one foot) over short distances.

a. Breakwater: Fourchon Beach

b. Jetty: Belle Pass

Figure 7.6. Photographs of Coastal Wave Features

c. Shoreline Armoring: Foreshore Protection Along Lake Pontchartrain

d. Shoreline Bulkhead

Figure 7.6. (continued) Photographs of Coastal Wave Features

7.4. Impact of Coastal Features Relative to the Surge Conditions

Crucially, the particular influences of coastal features are affected by the specific surge conditions. Drowning of a feature during extreme surge events significantly diminishes its impact, compared with its influence for smaller surges or tides alone. Employing the analogy of the drum of water spilled on the floor, the bulk of the spill can only be controlled by large continuous features—small raised bumps and cracks in the floor will not divert the water until the depth gets down to a thin film.

As noted earlier, the surge flow resistance and wave breaking by coastal marshes and forest underbrush are significantly affected by the degree submergence. (Forest trees themselves can be too widely spaced to influence surge but may reduce wave transmission and regeneration.) Simple reductions in surge per distance traveled over marsh—e.g., the old "rule of thumb" of one foot of surge reduction per 2.7 miles of marsh—are not reliable (Suhayda and Jacobsen 2007, Resio and Westerink, 2008).

Loder (2008) modeled the influence of marsh—bottom elevation, depth-independent friction, and continuity—on surge SWL and wave heights in an idealized domain. Loder found SWL reduction was highly sensitive to surge magnitude, even without taking into account Manning's *n* depth-dependency. Increasing *n* from 0.002 to 0.2 reduced inland SWL, but these reductions varied between 35 and 76% as levels of inundation were reduced. At constant *n* of 0.005, the SWL reduction varied between 2 and 52% depending on depth alone. However, H_s reduction over marsh was much less sensitive to surge magnitude, with consistent 60+% reduction.

Wamsley et al (2009) provided a preliminary assessment of the influence of marsh conditions on surge. Using the Caernarvon Marsh, the authors applied a simple fixed adjustment to the regional topography, and thereby modified the associated percentage of land cover types (based on elevation). The authors used three topographic/land cover scenarios (base, degraded, and restored). Due to the basic scope of their investigation they only used constant (not depth dependent) Manning's *n* values for each land cover type. They then compared surge results for two hypothetical hurricane simulations on identical tracks—a large moderate storm (similar to Hurricane Hilda) and a large intense storm (similar to Hurricane Katrina). Figure 7.7 shows the results for reduced peak surge and maximum waves for the base versus degraded condition. In this analysis, the degraded marsh had surge heights up to 90% higher, and maximum wave heights up to three feet higher, than the base condition for the intense storm. Given the basic analysis, the authors were not able to distinguish between the contributions of topography and land cover modifications. Additional research is needed on the effects of changing topography and land cover, incorporating depth-dependent Manning's *n*.

The role of coastal channels surrounded by expansive low-lying marsh in conveying surge is also stage dependent. An important and often misunderstood example is the influence of the coastal MRGO Reach 2, as compared to the interior Reach 1 (Figures 7.5k and l), during Hurricane Katrina (Jacobsen and Suhayda 2006, Ebersole et al 2010). Coastal channel conveyance is very significant during low to moderate surge events—as it is for typical tide and weather mediated exchange. However, during more extreme surges the vast majority of flow is likely to occur overland and the importance of the channel conveyance diminishes. Similarly, embankments and natural ridges can mitigate low-to-moderate surge but may provide very little reduction of extreme surges.

The lesser relative impact of certain coastal features on extreme surge is an important consideration in prioritizing wetland "multiple lines of defense" for urban surge protection, shown in Figure 7.8 (see Lopez 2008). Features which do not sufficiently contribute to high hazard protection may not warrant investment for urban flood protection. However, for less urbanized coastal communities, enhancement

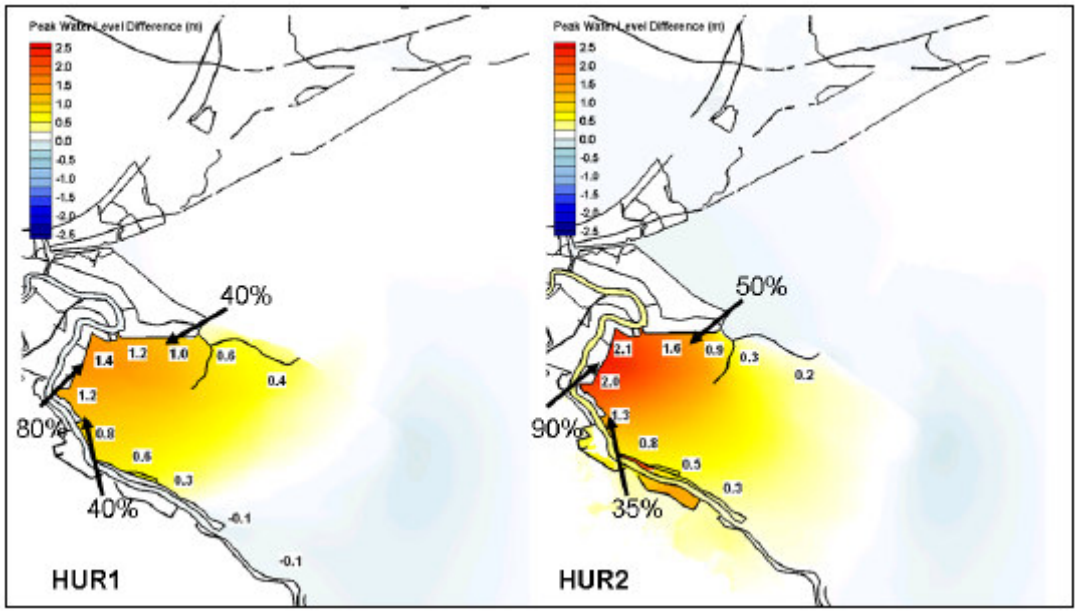

a. Peak Surge Difference

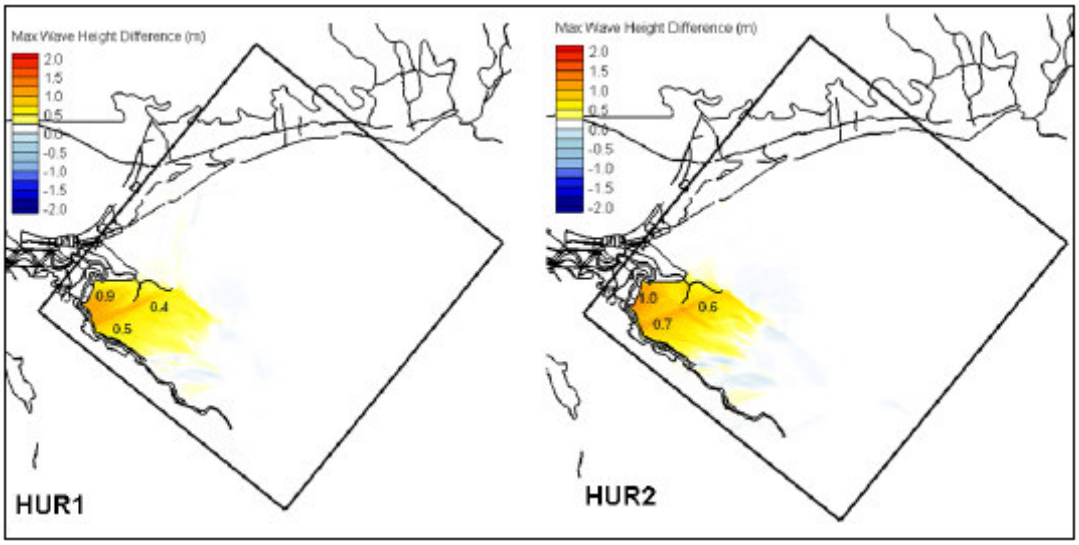

b. Maximum Wave Height Difference

Figure 7.7. Difference Between the Degraded and Base Caernarvon Marsh Conditions
Hurricane 1—Large, Moderate (Hilda); Hurricane 2—Large, Intense (Katrina)
(Wamsley et al 2009)

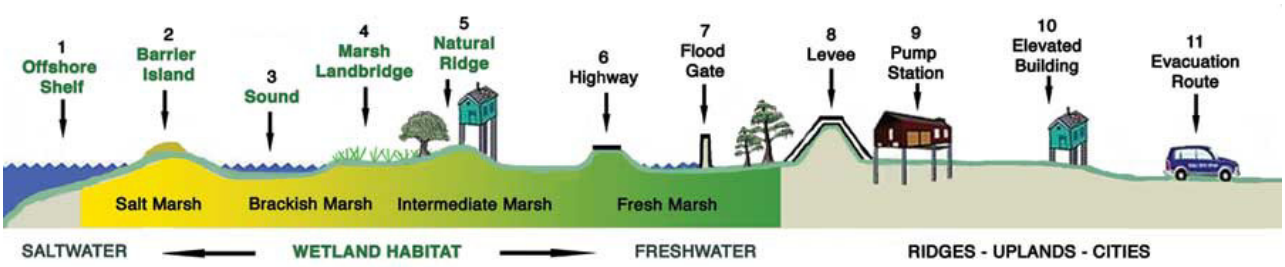

Figure 7.8. Multiple Lines of Defense Strategy
Lopez 2008

of low-lying features may provide cost-effective protection against lower (typically more frequent) surges. Low-lying features may also be cost-effective in mitigating the assaults of recurring modest surges on fragile ecosystems, such as shoreline erosion and saltwater damage along the MRGO Reach 2.

Massive urban surge protection systems can have significant negative coastal ecosystem impacts. The higher setup created by these systems (see Figure 6.3.d) can alter coastal circulation, erosion, and deposition patterns associated with storm surges. An example is the erosion in the Canaervon Marsh during Hurricane Katrina. Depending on their design, these systems can also disrupt normal estuarine tidal flow and water quality (e.g., see discussions regarding the proposed Morganza to Gulf Project, http://www.mvn.usace.army.mil/prj/mtog/feasibility_study_documents/mtog_index.htm).

Importantly, coastal features can have very different impacts depending on a storm's track and associated surge orientation. Surge setup against Grand Isle was from Barataria Bay (on the north side of island) during Hurricane Katrina, but from the Gulf of Mexico (on the south side) during Hurricane Gustav. Thus, shoreline breakwaters, enhanced dunes, and other features on Grand Isle have different impacts depending on whether surge is approaching from the north or south.

Impacts can also vary over the course of a storm as wind direction reverses. Prior to its closure at Bayou La Loutre, the MRGO Reach 2 (Figures 7.5c and k) conveyed early surge from Breton Sound toward New Orleans. But at the time surge peaks at the confluence with Reach 1 and the GIWW (called "the funnel," Figure 8.4l), Reach 2 conveyed surge outward to Breton Sound (see Jacobsen and Suhayda 2006). Figure 8.9 illustrates the reversal in the SWL difference along Reach 2 with and without Reach 2 closure for a storm similar to Hurricane Betsy (the green line is the headloss without the closure, the orange line is with the closure). The headloss reverses several hours prior to the peak at the upper end of Reach 2 (at the Paris Road Bridge). In this example Reach 2 closure raises peak SWLs in upper Reach 2 (the red line peak is higher than the blue line peak). As expected though, the effect of Reach 2 closure in raising the Paris Road peak SWL is small given that most of the regional conveyance is outside the MRGO. (The analysis was done prior to construction of the IHNC Surge Barrier.)

The complexity of surge-landscape interactions means that careful analysis is required in planning for coastal improvements.

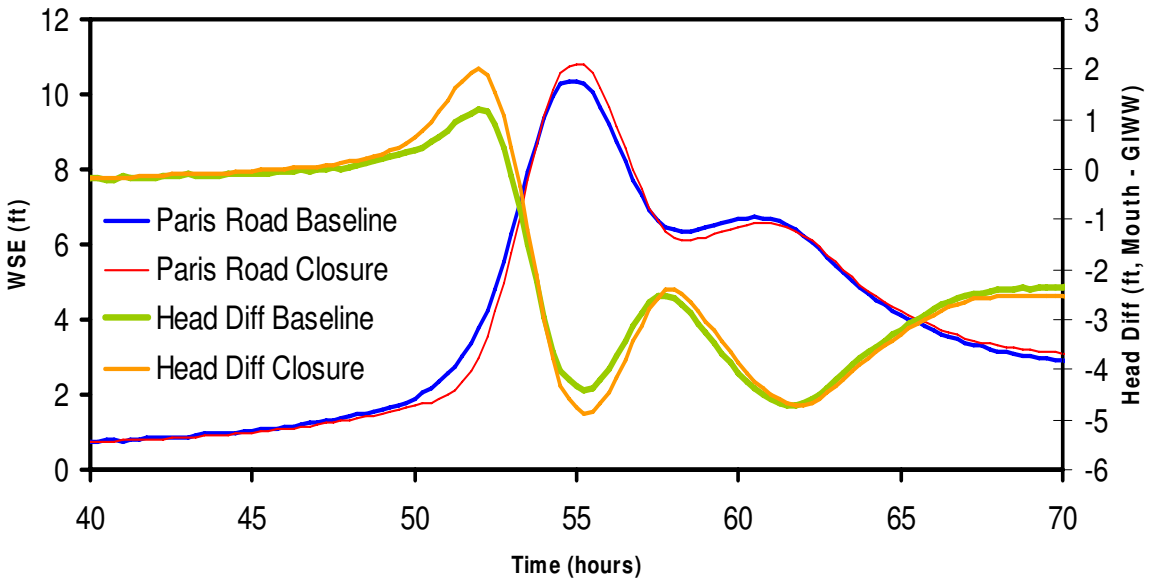

Figure 7.9. Changes in Paris Road SWL and MRGO Reach 2 Headloss with Reach 2 Closure for Betsy-Like Hurricane
(prior to construction of IHNC Surge Barrier)

Subpart B. Hurricane Surge Modeling

Leading scholars in the field of coastal hydrodynamics have developed sets of mathematical equations to capture the physics-based descriptions of hurricane surge dynamics presented in Part II Subpart A. To solve these equations in the context of subtle surge-landscape interactions they have researched methods for producing highly detailed representations of coastal conditions (e.g., topography and friction at a scale of tens of meters). Scholars have also addressed the severe numerical, coding, and computational challenges associated with solving time-varying surge SWL and wave equations for a large high resolution domain. One key advancement has been the porting of models to High Performance Parallel Computing (HPPC) systems. Together, these hydrodynamic equations, landscape representations, codes, and numerical and computational methods constitute what are called hurricane surge models. Furthermore, since all models are necessarily approximations of actual surge phenomena,[1] scholars have examined the effects of simplifying physics (e.g., ignoring buoyancy forces), generalizing landscape conditions (e.g., smoothing terrain), and selecting particular computational techniques.

Following the disastrous hurricane seasons of 2004-05, which saw seven major hurricanes in the Gulf of Mexico, four of which made landfall at major status along the CN-GoM, practical applications of high resolution surge modeling have been sought by surge risk managers, including those at FEMA (for FISs), the USACE (for flood protection and coastal restoration planning and design), and other public agencies and private parties. Governmental agencies have partnered with universities and the engineering community to provide modeling approaches which satisfy project requirements. These partners are also continuously working to improve modeling techniques.

This Part II Subpart B discusses the following topics:

> Section 8., technical approaches and general issues associated with high resolution modeling of surge SWL physics;
>
> Section 9., technical approaches and general issues associated with high resolution modeling of surge wave physics;
>
> Section 10., the ADvanced CIRCulation (ADCIRC) model—and its coupling with wind field and wave models—which FEMA and the USACE primarily rely on to characterize surge and wave hazards throughout the Gulf of Mexico and South Atlantic; and
>
> Section 11., recent applications of high resolution surge models and quality of hindcast results.

These sections address both current and evolving methodologies in high resolution modeling. A key source of information for these sections is a recent summary by Jacobsen et al (2010) for FEMA

The reader is encouraged to consult GTN-1 for an introduction to concepts involved in evaluating model accuracy and precision, and sensitivity, calibration, and validation testing for model performance.

The ensuing Part III addresses how information on regional hurricane climatology (presented in Part I) is combined with surge modeling (addressed herein) to provide hurricane surge return frequency analysis.

---

[1] The famous saying: "essentially, all models are wrong, but some are useful," (by the statistician George E. P. Box) emphasizes the point that models have to simplify reality to some degree and their potential weaknesses in accuracy and precision (see GTN-1) should be understood before employing them.

Section 8. SWL Modeling

8.1. General Background

Hurricane surge SWL (or η) modeling is an extension of coastal hydrodynamic modeling for tidal and meteorological driven circulation. *History of Coastal Inundation Models* (Massey et al 2007) reviews the evolution of these models. FEMA in support FISs, NOAA in support hurricane emergency evacuation and response, the USACE for planning hurricane protection systems, and the Navy for support of nearshore operations have been the principal sponsors for the development and application of surge SWL models in the United States. These agencies frequently coordinate on aspects of surge modeling, funding leading university researchers and sharing code developments. In particular, the USACE—through its Coastal and Hydraulics Laboratory (CHL)—has worked closely with FEMA on regional surge studies (such as the surge hazard analysis for southeast Louisiana).

The hurricane wind field is the primary force responsible for generating surge SWLs and waves, with atmospheric pressure deficit and wave radiation stress gradients also contributing to η. Hurricane SWL and wave modelers typically use NOAA H*Wind files—as described in Part I—and atmospheric pressure data to perform hindcasts, including those undertaken for sensitivity, calibration, and validation testing. For synthetic hurricane surges, modelers create wind and pressure fields with vortex models—also described in Part I—which are based on inputs for the track, the central pressure deficit (CPD), the radius to maximum winds (R_{max}), the wind field profile (Holland B), asymmetry, intensification, and decay. Uncertainties with H*Wind files and vortex models can have a major influence on surge modeling results, as wind setup is proportional to wind velocity squared. Thus, a ten percent error in wind speed can easily translate into a twenty percent error in the estimated setup.

Currently, surge hazard analysis employ surge models representing 2D physics using one equation for mass conservation and two for momentum (one for the east-west, x, direction and one for the north-south, y, direction). The three equations are known as the Shallow Water Equations (SWEs), and are partial differential equations written in the mathematical language of calculus. Specific formulations are developed to incorporate the various terms (described in Section 6) and used to solve for the three dependent variables throughout the geographic domain over which surge is being evaluated: the SWL setup (η) and two depth-averaged velocity components (u and v).[1]

Surge SWL modeling requires translating the SWEs into numerical approximations—using finite algebraic terms—that can be solved with a computer. The algebraic equations are incorporated into engineering software code that simultaneously solves for η and depth-averaged u and v at each surge water column, for any point time. These models are termed *dynamic* (or *unsteady, transient,* or *time-dependent*) as they seek to describe conditions as they vary during the course of the event.

2D surge codes simulate hydrodynamic processes—which are *naturally continuous,* spatially and temporally—as a series of *artificially discretized* spatial and temporal steps. The lateral spatial intervals

[1] In ocean physics the 3D Navier-Stokes equations form the basis for a complete physical analysis. The SWEs, also known as the Saint Venant equations, are derived from the 3D Navier-Stokes equations assuming hydrostatic conditions, negligible, baraoclinic forces, and applicability of depth-averaging (for example, see Dawson and Mirabito, 2008). 3D analysis is primarily the focus of academic research (e.g., under funding by the U.S. Navy Research Laboratory, NRL, and other agencies). A full 3D analysis may reveal localized variations in surge SWL not described in 2D, such as those associated with sharp vertical gradients in salinity and temperature driven buoyancy forces (Weisberg and Zheng 2008, Resio and Westerink 2008, Dresback et al 2010, Weaver and Luettich 2010, Sheng et al 2010).

(the columns) are defined by points, termed nodes. Modelers create a data file containing the node locations in a horizontal coordinate system (e.g., latitude/longitude).

Starting with an initial condition, the 2D code computes SWL and velocity vectors at each node at each subsequent specified time-step as a function of the translated equations and five sets of input values:

1. Initial conditions, i.e., the starting water surface elevation and velocity (x and y) throughout the domain (at each node);
2. Lateral boundary conditions, i.e., the water surface elevation or velocity for those nodes along the perimeter, which must be specified for all time-steps. These include river flows into the domain and the tides at the open ocean boundary.
3. SWL gains/losses (rainfall, evaporation) at each node.
4. Forces with specified magnitudes (e.g., gravity) at each node.
5. Nodal attributes governing unspecified force magnitudes, such as bathymetric/ topographic elevation of each node, the friction coefficient, the eddy viscosity coefficient, the wind sheltering coefficient, and the air-sea drag coefficient.

Depending on the code, node inputs can be spatially uniform or variable, as well as temporally constant or variable. Spatially and temporally variable inputs can themselves be computed according to a specified rule (code subroutines) using other inputs (e.g., date/time dependent tides, latitude dependent Coriolis force), the current solution (e.g., depth dependent friction coefficient, velocity shear dependent eddy viscosity), or coupled models (e.g., atmospheric pressure and wind speeds from a vortex model and radiation stress gradients from a wave model). The influence of major uncertainties in input values (e.g., friction coefficient, wind field, etc.) are assessed with sensitivity analyses (see below).

8.2. Model Numerical Methods

Discretization of space and time leads to two fundamental modeling challenges. The first challenge is determining the number and spacing of nodes to represent the physical domain, which is akin to selecting the megapixel resolution for a digital camera. Node arrangements vary in the fidelity of their representation of the real domain terrain and landscape properties (e.g., friction and other coefficients). In principle, higher resolution supports better surge modeling detail and accuracy, but at the expense of greater computational resources. However, some surge models may not improve with greater terrain and landscape detail, due to other uncertainties or model limitations, just as poor lighting can obviate the advantage of a higher resolution digital camera.

The second challenge is devising the algaebraic algorithms for solving conditions at each node which approximate the PDEs. Numerical translations of surge PDEs are equations with an infinite series of algebraic terms, usually listed in order of greater accuracy refinement. All numerical methods must choose a point at which to truncate these translations, introducing what is termed as truncation error. Higher order solutions necessarily include more terms and less truncation error, but are more computationally expensive. Solutions with only “first order” accuracy have a truncation error that typically introduces significant artificial smoothing (also termed numerical dissipation or dampening). “Second order” solutions have higher accuracy but less dampening, and consequently are more susceptible to instabilities—spurious errors which can become compounded over time. The algorithms are analogous to computer animation tools which apply rules of motion to a still frame. The more rules of motion—tailored to each object in the still frame and to the changing conditions of each object—the more realistic the animation.

Simple domains can be modeled with *structured grids* composed of rectangles or smooth regular curvilinear quadrilaterals. Structured grids accommodate the generally more direct numerical solutions known as *finite difference* methods. Two well known codes which rely on structured grids and finite difference numerical methods are Sea, Lake, and Overland Surge from Hurricanes (SLOSH), which is often used by NOAA and the USACE in emergency planning, and FEMA Surge, which was formerly used in coastal FISs. Figure 8.1 illustrates a structured curvilinear grid for southeast Louisiana.

The alternative to a structured grid is an unstructured grid, or mesh. A triangular (or quadrilateral) mesh can have tighter (i.e., denser) node spacing along irregular coastlines, interior floodplains, and raised topographic features to better resolve physical processes in these areas. Conversely, the same mesh can have coarser spacing over areas where de-resolving hydrodynamic processes is suitable (e.g., the open ocean and flat expansive marsh). By employing variable node spacing, unstructured, triangular meshes can better optimize the location and number of nodes to represent complex coastal domains. Figure 8.2 illustrates an unstructured triangular mesh.

Solutions for an unstructured mesh require less direct, more sophisticated *finite element* numerical methods. Finite element methods encompass a range of approaches but typically have greater computational requirements for a given number of nodes. However, for a given target refinement in an area of interest, the unstructured mesh may contain significantly less nodes, in which case the combination of the unstructured mesh and finite element method may be more computationally efficient. Finite element methods have been routinely applied to floodplains for two decades to cost-effectively capture complex hydrodynamic patterns. The combination of an unstructured mesh with the finite element method has become more attractive in the last ten years as computational costs have drastically declined and the demand has increased for better resolution of domain landscape features.

Both finite difference and finite element numerical methods are designed to conserve mass over the global domain at each time step within machine precisions. However, an important difference is that finite difference methods conserve mass on a node by node basis, while finite element methods conserve mass over patches of nodes. The absence of strict mass conservation at the node level in the finite element method is not typically a problem unless sources of instabilities are present (see below) or surge flow become supercritical (e.g., shallow flow down steep slopes). The unstructured mesh for a finite element model can be further refined to improve mass conservation (to an acceptable tolerance) over particular small areas of interest, and remain (depending on the degree of refinement) more computationally efficient than a corresponding finite difference model. A third type of numerical scheme, *finite volume*, employs unstructured meshes but imposes strict mass conservation over each triangular mesh element (e.g. FVCOM, ADCIRC-DG). However, finite volume methods are much more computationally demanding, and without higher order numerical schemes tend to introduce considerable dampening.

Finite difference and element methods can be either fully explicit, fully implicit, or a blend. Explicit methods solve the 2D equations for SWL and velocity at each node for the current time-step solely based on results from the previous time-step; i.e., the current time-step solution is only dependent on

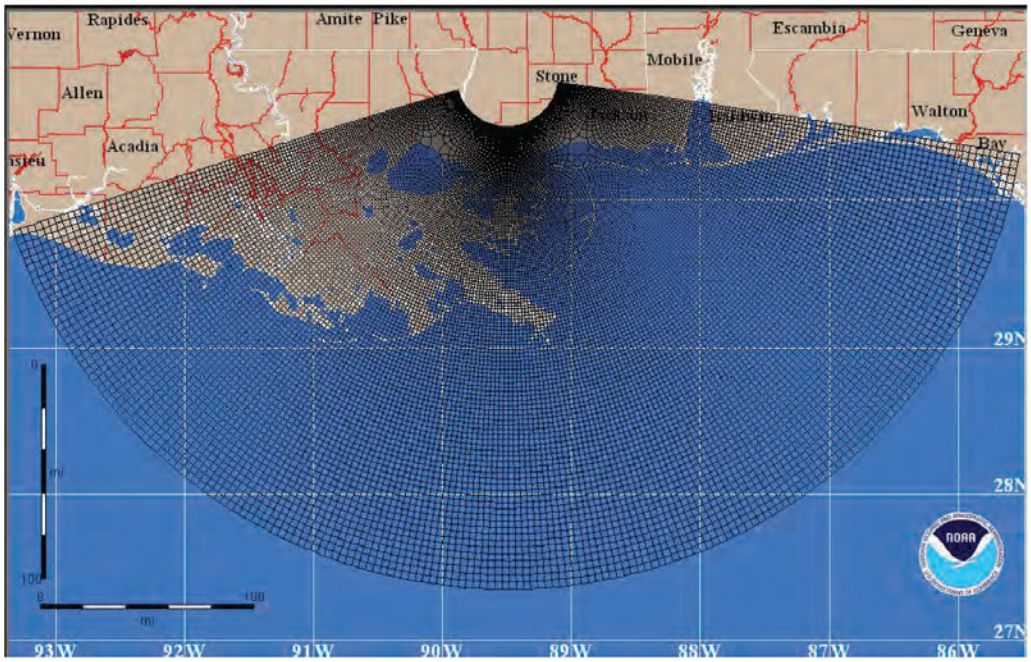

Figure 8.1. Example of a Structured Curvilinear Grid
Glahn et al 2009

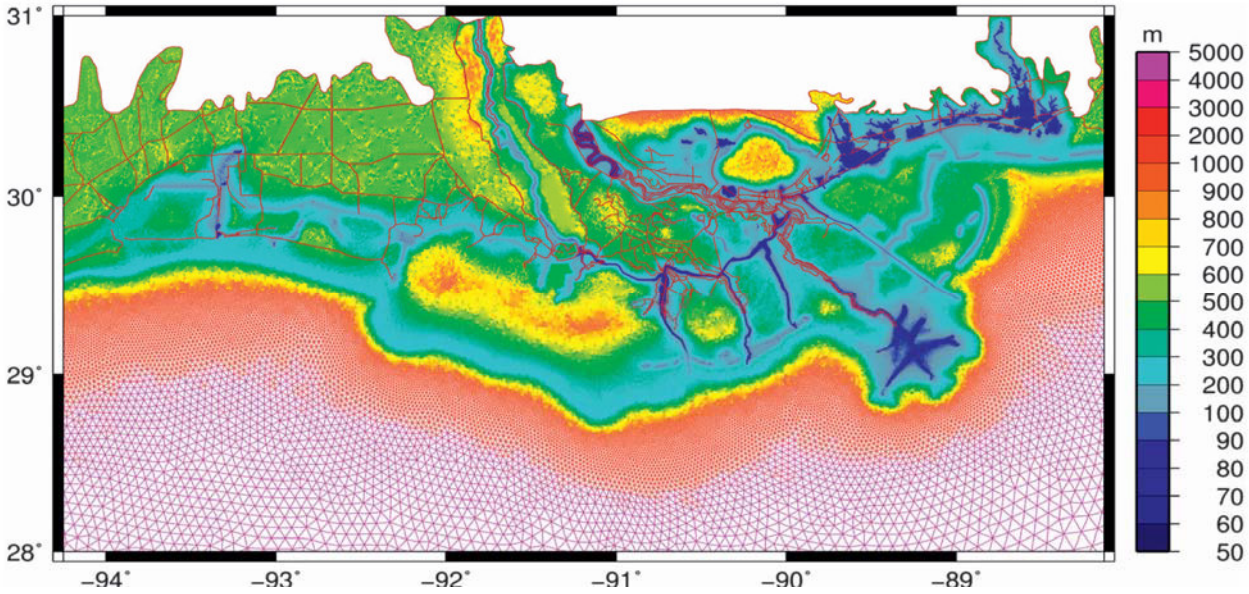

Figure 8.2. Example of an Unstructured Grid, or Mesh
(Legend is node spacing)
Bunya et al 2010

pre-determined values. Implicit methods solve equations for SWL and velocity at each node by also incorporating results for adjacent nodes at the current time-step. These latter values are obviously not determined prior to the model marching to the current time-step. In contrast to explicit methods, implicit methods require the use of more computationally intensive iterative techniques (which in turn require specification of iteration limitations and/or convergence criteria). Explicit methods are subject to Courant instabilities while implicit methods can be strained by wetting and drying fronts (see below).

With declining computer processing costs, 2D hydrodynamic codes are being been written to take advantage of parallel computer processing architecture. Some codes can only use the additional processors on a single workstation, while others can be used with High Performance Parallel Computing (HPPC) systems employing hundreds of computer cores. Academic research of surge hydrodynamics has utilized HPPC systems for nearly a decade (Westerink 2004). Since the destructive 2005 hurricane season, HPPC systems have seen wider practical application in FEMA and USACE surge modeling due to increased availability, speed, and cost-efficiency of the HPPC systems, as well as the demand for higher spatial and temporal resolution of surge physics, which requires vastly more computational steps.

Table 8.1 provides a list of 2D hydrodynamic codes which have been applied to regional scale, high resolution hurricane surge studies and notes several key characteristics and limitations. (Codes that are applied primarily to local-scale studies, such as bridge scour evaluations, are not included.) The code providers noted in Table 8.1 continue to work on a range of improvements, including 3D physics; full baroclinic forcing; better parameterization of turbulence stress and friction; updates to wind vortex models; coupling with wave models (see Section 9); more robust wetting and drying schemes; more efficient and accurate numerical methods; and better computational efficiency. One recent advancement in two finite element codes (ADCIRC and ADH) is automatic mesh refinement to enhance local mass conservations and restrict local instabilities.

8.3. Node Attribute Data

Modelers require domain geometry (topographic and bathymetric) and land cover data in order to establish node elevations and coefficients for wind sheltering and friction. Modelers typically obtain these data at two scales: large coverage (e.g., at scales of U.S. Geological Survey, USGS, quarter quadrangle to county-wide) and feature-specific (e.g., at scales of particular water bodies and land features). Large coverage topographic data sets are increasingly available through federal-state-coordinated efforts (e.g., USGS, NOAA, and FEMA sponsored topographic data and digital elevation models, DEMs, derived from Light Detection and Ranging, LIDAR). Coordinated survey efforts produce data and DEMs for regional bathymetry. The U.S. Fish and Wildlife Service (USF&WS) and other agencies sponsor updates to the National Land Cover Data (NLCD). Large coverage sources typically provide the bulk of the required data.

Key coastal landscape features (see Section 7) may not be adequately represented in large coverage data sets. Large coverage data sets may be outdated—such as with an accreted shoal, eroded shoreline or barrier island, urbanized landscape, dredged channel, expanded jetty, etc. In some cases, the large coverage data may be current but may not adequately resolve small features with potential significant impact, such as a LIDAR DEM not capturing the height of a floodwall crest. In these instances mesh development and attribute assignment need to incorporate feature-specific geometry and cover information. Some coastal features require detailed investigations and surveys to provide adequate node information.

Table 8.1. 2D Hydrodynamic Codes for Hurricane Surge SWL Studies

Code	Developer	Open Source	Wave Setup	Numerical Method	HPPC Compatible	Licensing
Adaptive Hydraulics (ADH)	ERDC USACE	Yes	Yes; loose coupling with wave model (e.g., STWAVE)	Finite element with adaptive mesh	Yes	Parallel version licensed from USACE (CHL)*
Advanced Circulation (ADCIRC)	ADCIRC Development Group	Yes	Yes, tightly coupled version with SWAN	CG - Finite element; DG -finite volume with adaptive mesh and numerics	Yes	Parallel version licensed from USACE Coastal and Hydraulics Laboratory (CHL)/ADCIRC Development Group*
Coastal Modeling System M2D	ERDC USACE	Yes	Yes; loose coupling with STWAVE	Finite difference	Yes	Parallel version licensed from USACE (CHL)*
Delft	Deltares	Yes	Yes	Finite difference	Yes	Licensed from Deltares
FEMA Surge	FEMA	Yes	No	Finite difference	No	Not in general use since the 1990s
Finite Volume Coastal Ocean Model (FVCOM)	University of Massachusetts, Dartmouth	Yes	Yes; tightly coupled version with SWAN	Finite volume	Yes	Not licensed for commercial applications
MIKE21	Danish Hydraulic Institute	No	Yes	Finite difference or finite volume	Limited to cores on workstation	Must be purchased from DHI
Regional Ocean Modeling System (ROMs)	Rutgers Ocean Modeling Group	Yes	Yes; tightly coupled version with SWAN	Finite difference	Yes	Free license including commercial applications.
Sea, Lake, and Overland Surge from Hurricanes (SLOSH)	FEMA/USACE/ NOAA	Yes	No	Finite difference	No	Generally shared within the emergency planning community for establishing flood envelopes; not typically available for commercial applications
SELFE	Oregon Health and Science University	Yes	Yes; coupled with WaveWatch Model II	Finite element	Yes	Free license including commercial applications.
Telemac	The TELEMAC Consortium	Yes	Yes; coupled with TOMAWAC	Finite element	Yes	Free license including commercial applications.

*Serial version licenses can be obtained with Surface-water Modeling System (SMS) user interface software from Aquaveo, LLC.

Source data for the nodal attributes should be:

- Complete with regard to the domain;
- Representative of conditions appropriate to the hurricane being simulated (e.g., historic landscape conditions for Hurricane Betsy; late summer/early fall vegetation conditions for synthetic storms);
- Accurate, with acceptable limits of uncertainty;
- Sufficiently spatially resolved to support interpolation to the particular mesh node spacing;
- Compatible, in cases where multiple, overlapping data sources must be used.

Limitations in nodal attribute data are often a major source of model inaccuracy and overcoming them requires substantial effort during model development. For example, topographic/bathymetric elevation data from numerous sources having different applicable dates, vertical references, and levels of uncertainty must be reconciled. (GTN-2 discusses issues related to appropriate vertical referencing for coastal Louisiana.)

Figure 8.3 illustrates some nodal attribute data for the unstructured mesh shown in Figure 8.2

8.4. Instability Issues

The very nature of numerical methods (simplified algebraic approximations of complex PDEs, spatial/temporal discretization, truncation of higher order terms, precision limits, convergence criteria, iteration restrictions, etc.) entails accuracy limitations. Furthermore, as a model progresses through time-steps computational methods can cause mass conservation errors at particular nodes to compound drastically, creating local solution instabilities and extremely unphysical results (e.g., high “mountains” or low “depressions” in the water surface). As the simulation proceeds, some instabilities can create mass conservation discrepancies large enough to exceed the modelers preset tolerance for terminating the simulation. “Non-fatal” instabilities can propagate below termination tolerances, “contaminating” local results, and can only be identified by a careful inspection of output. Figure 8.4 presents peak surge elevation profile along an inland river and illustrates an instability in an implicit versus an explicit simulation.

Modelers can try four “quick fixes” to reduce model instabilities.

1. Select a different numerical method or scheme (e.g., explicit versus implicit).
2. Alter the treatment of one or both momentum terms. For example, removal of acceleration terms in the momentum equation would impose a pseudo steady, gradually varied flow solution. However, this would not be suitable for depicting large, rapid surges through narrow inlets.
3. Reduce the model time-step. However, reducing the time step increases model runtime, roughly proportionately.
4. Increase the nodal eddy viscosity value (see Section 6). Higher eddy viscosity values boost local momentum diffusion, smoothing local velocity gradients (see below). However, higher eddy viscosity values can lead to unrealistically sluggish hydrodynamics.

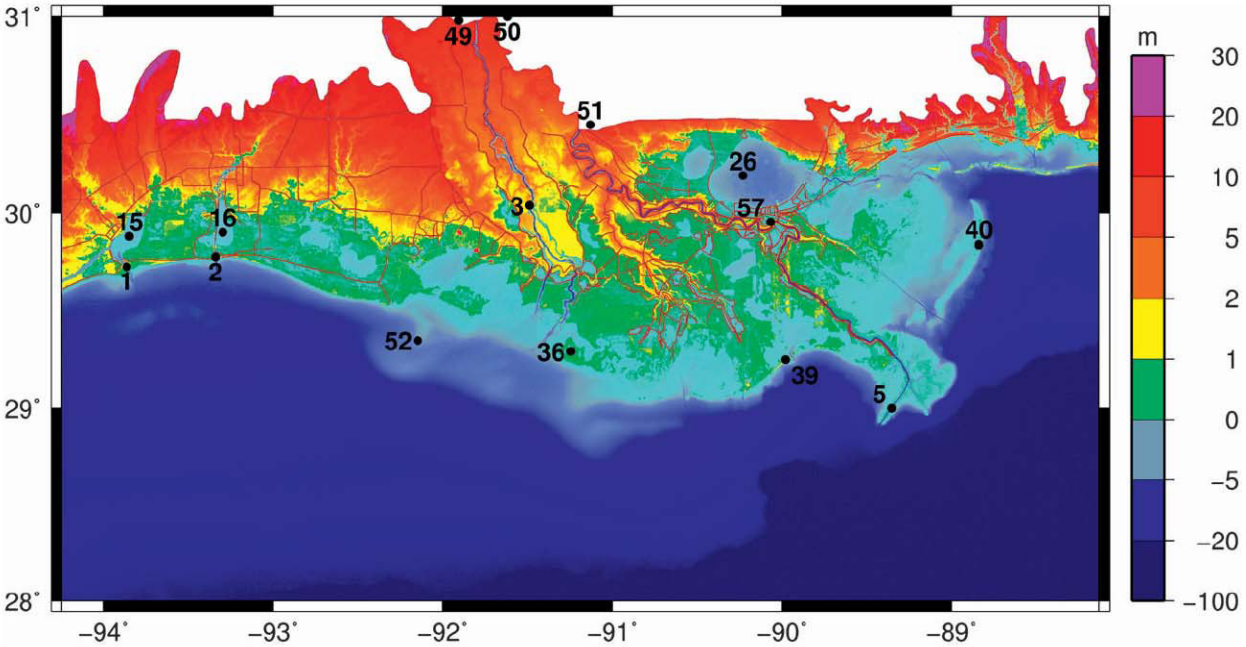

a. Topography and Bathymetry

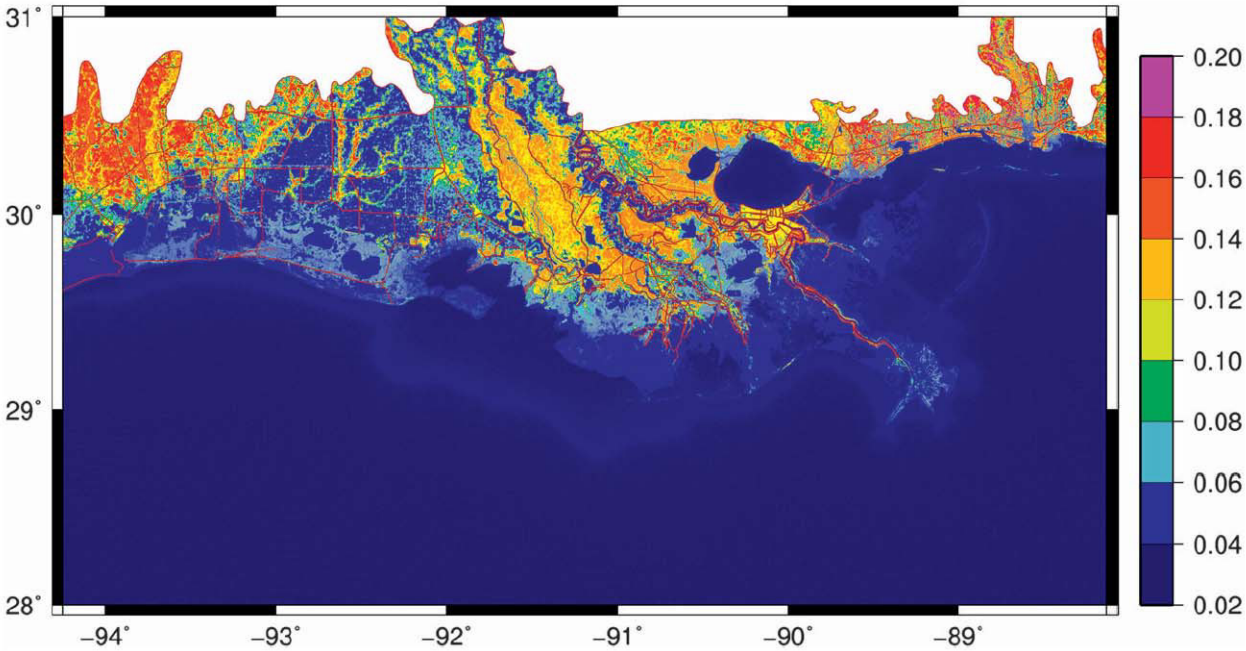

b. Manning's n Friction Coefficient

Figure 8.3. Example of Node Attributes for Unstructured Mesh
Bunya et al 2010

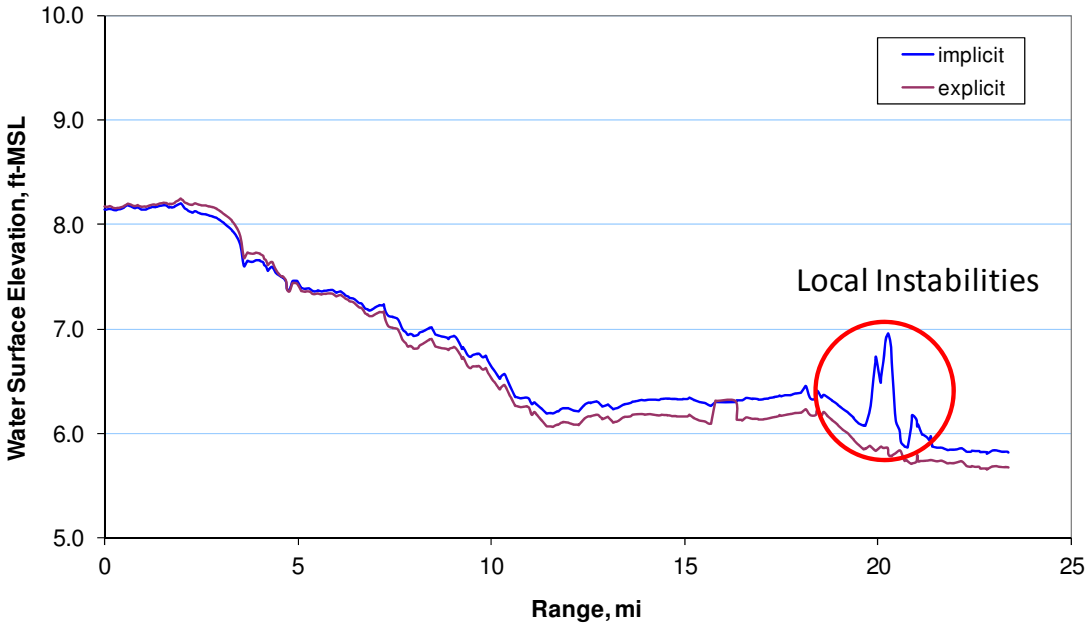

Figure 8.4. Example of Instability in an Implicit versus and Explicit Simulation Comparison of Peak Surge Elevation Profiles Along an Inland River
Jacobsen et al 2010

To avoid the potential drawbacks associated with these quick fixes, experienced modelers will usually investigate potential mesh sources of instabilities and make revisions to mitigate them. Four significant sources of instability associated with mesh arrangements and their potential solutions include:

1. The Courant stability condition. This condition, critical with explicit numerical schemes, requires that the maximum physical velocity at which a perturbation in the SWL (e.g., a wave) propagates be much less than the velocity at which the numerical solution propagates (node spacing / time-step, or *dx/dt*). Surge perturbation velocity in nearshore areas and overland is the same as shallow water wave celerity [$(gh)^{½}$ where *h* is water depth]. The value of $(gh)^{½} * (dt/dx)$ should generally remain less than 0.5 throughout the model domain and over the course of the simulation. For example, at dt = 1 s, the value of $(dx)^2/h$ (units of feet) should exceed 130. Thus, improving Courant stability requires mesh de-refinement or time-step reduction.

2. Mesh quality. Numerical stability in unstructured meshes is improved by using mild area transitions between adjacent elements and by avoiding small interior angles (i.e., for triangles the more nearly equilateral the better). The former requirement tends to increase node density while the latter tends to decrease it.

3. Force and velocity gradients. Solutions with smooth force and velocity gradients tend to remain stable. Smoothness is improved by a) designing meshes with element edges that follow attribute contours (e.g., elevation, Manning's n, and other attributes affecting force generation); and b) reducing perturbations in, and the steepness of, attribute gradients (i.e., smoothing the contours); and c) refining the mesh in areas of high gradients. Approaches a) and c) tend to increase mesh resolution, while b) tends to decrease mesh resolution.

4. Wetting and drying fronts. Wetting and drying are a significant source of instabilities in surge modeling (See Dietrich et al 2005, and Massey and Blain 2008). 2D models can advance wetting/drying fronts subject to certain thresholds—e.g., water depth and velocity. These logical (on-off) conditions help to control wetting/drying oscillations, which numerical methods can exacerbate. Models, however, must also avoid steep, irregular wetting/drying fronts. The three approaches to alleviating steep, irregular velocity gradients can also be used to address problematic wetting/drying.

In addition to adjusting the mesh and nodal attributes to relieve these force gradient and wetting/drying sources of instabilities, the modeler can use refinement to impose greater local mass conservation. However, in refining a mesh, the modeler must recognize that the Courant condition may require a time-step reduction, particularly for mesh refinement in areas of deeper water. If reducing the time step is not practical, the modeler may need to coarsen the mesh and smooth the attribute gradient. Models with longer time-steps and coarser meshes often have much lower development and production costs, and faster schedules, but sacrifice domain fidelity and possibly simulation accuracy.

Model codes with higher numerical accuracy—i.e., lower truncation error and thus lower numerical dampening—will typically face more instability problems. However, such codes provide the modeler with control over optimizing model stability with fidelity to terrain and land cover conditions. This optimization involves extensive manual adjustments to node positions and attributes, which are extremely tedious and time consuming. Testing these adjustments can require numerous simulations.

8.5. Model Performance Testing

GTN-1 provides an introduction to testing of model performance for accuracy (bias) and precision (uncertainty)—including sensitivity, calibration, and validation testing. Due to complex surge dynamics, performance evaluation of surge models requires high quality surge data—both for HWMs and hydrographs—over a broad area. However, federal and state agencies have not had adequate plans for collecting such data until recently. For southeast Louisiana, data prior to 2005 have also had significant problems with vertical referencing (see GTN-2).

Surge model performance is also typically evaluated for tides, as there is usually greater availability of numerous high quality tide time series compared to surge events. Modelers usually evaluate the tidal constituents themselves, which requires harmonic analysis of tide station data. Importantly, inshore areas are likely to be much more sensitive to conveyance conditions for evaluations of tidal propagation versus extreme surge events. Modelers must therefore consider potential differences in bottom friction (e.g., Manning's *n*) for tides versus surge events.

Surge SWL model sensitivity tests examine the relative influence of various model settings (e.g., mesh layout, modification of acceleration terms, time-step), initial and boundary conditions, and inputs (e.g., nodal attributes, wind values, etc.) on the model efficiency (i.e., runtime), stability, and the quality of results. Thus, sensitivity tests provide important information on what is called model robustness: the simulation conditions for which particular settings and parameters can be applied. Sensitivity tests can use actual tide and surge events or hypothetical/synthetic conditions. When employing the latter the tests are often termed "numerical experiments."

Calibration tests simulate actual tides and surge events. The modeler compares the simulation results for SWLs and velocities to the observed values and adjusts parameters (those which have been found to be highly sensitive) within accepted ranges to achieve a best fit. Calibration often requires judgment on whether or not to "tune" a parameter—such as the friction coefficient (Manning's *n*)—to improve the

simulation of a particular event. For example, it may not be appropriate to apply a shallow marsh Manning's *n* value that supports tidal calibration to extreme surge events.

Following calibration, a validation test is performed on an additional separate hindcast to assess the selected settings and parameters. If the model is not calibrated, the validation test relies on the modeler's experience and judgment (based on previous models) for settings and parameter values. As discussed in GTN-1, validation results are used to identify model bias (inaccuracy) and precision (uncertainty). In employing the validated SWL model to simulate a range of possible hurricane scenarios any residual bias requires application of suitable correction factors (Dean et al 2004).

Models which employ coarse structured grids and finite difference codes (e.g., SLOSH), and which simplify surge physics by ignoring wave setup, have the advantage of being very simple, fast, and inexpensive to operate (e.g., simulating a few storm days on a desktop computer in less than an hour).[2] Figure 8.5 plots simulated versus observed SWL for the SLOSH model over several storms. The results show that SLOSH hindcast models can simulate SWLs above 15 ft within ±20% but are less accurate for lower surges, where detailed landscape features become important.

Models which incorporate a fuller physical description (e.g., wave setup) and higher resolution, may require hundreds of computer cores to simulate the same event, but usually provide better validation results, particularly at the lower SWLs affected by the coastal landscape. Figure 8.6 illustrates the ADCIRC model validation results for Hurricanes Katrina.

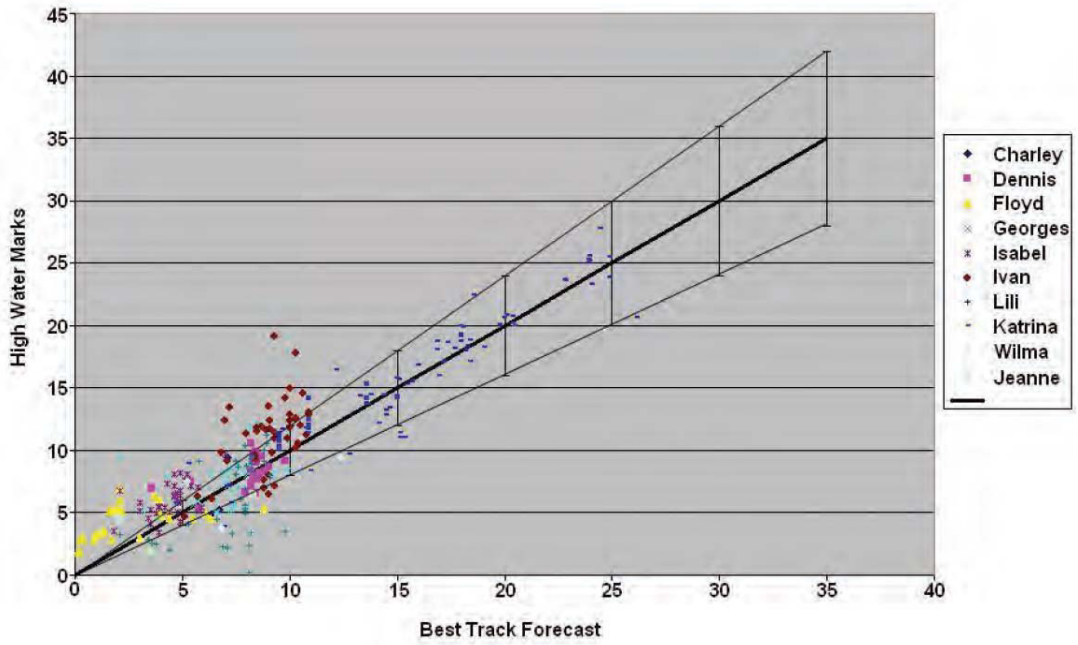

Figure 8.5. Comparison of SLOSH Model Predictions to Observed High Water Marks (With ±20% Error Bands)
Glahn et al 2009

[2] Due to rapid run-time demands and other exigencies, application of surge models like SLOSH to real-time forecasting, necessitates greater simplification than planning/design applications. A detailed discussion of simplifications in real-time surge forecast techniques, and their implications, is beyond the scope of this report

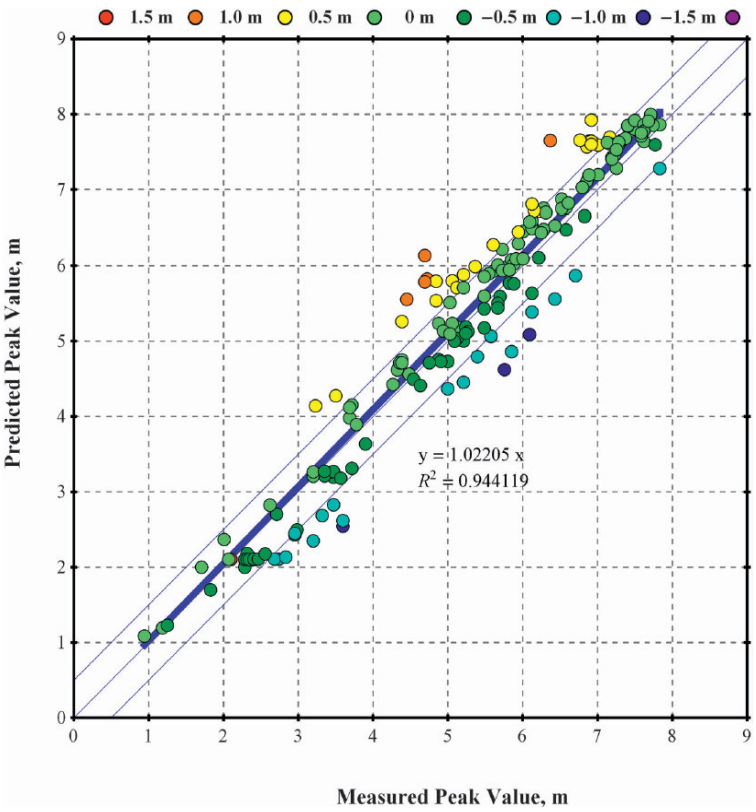

Figure 8.6. Comparison of ADCIRC Model Predictions to Observed High Water Marks Hurricane Katrina (With ±0.5 m Error Bands)

Bunya et al 2010